

Cite this: *RSC Appl. Polym.*, 2026, **4**, 466

# Detection, identification, and quantification of polymer additives: a review of techniques, approaches, challenges, and a possible roadmap in analysis

Tanmay Rahman,<sup>a</sup> Daniel Meadows,<sup>a</sup> Ke Zhan,<sup>b</sup> Harrish Kumar Senthil Kumar,<sup>a</sup> Marshall Smith,<sup>c</sup> Virginia A. Davis,<sup>a</sup> Bryan S. Beckingham,<sup>a</sup> Yucheng Peng<sup>b</sup> and Edward Davis<sup>b</sup> \*<sup>c</sup>

The type and concentration of additives in polymer systems play a crucial role in determining the physical, mechanical, and chemical properties of these materials, as well as influencing their processing and performance in end-use applications. However, polymer additive detection, identification, and quantification are challenging due to the very low concentrations used and the poor solubility of some additives in solvents required for testing. In addition, polymer degradation products can interact with the additives during testing. To address these challenges, various techniques have been developed. Each method offers unique advantages and challenges, including sensitivity, specificity, and limitations in the polymer systems to which it is applicable. Understanding the advantages and limitations of these methods is essential for selecting the appropriate technique for the polymer additive system under analysis. This article reviews the primary methods used for polymer additive detection, identification, and quantification, including Fourier transform infrared (FTIR) spectroscopy, Raman spectroscopy, nuclear magnetic resonance (NMR) spectroscopy, gas chromatography (GC), mass spectrometry (MS), high performance liquid chromatography (HPLC), carbon/hydrogen/nitrogen/sulfur (CHNS) analysis, inductively coupled plasma (ICP) analysis, energy dispersive X-ray spectroscopy (EDS), thermogravimetric analysis (TGA), differential scanning calorimetry (DSC), and X-ray diffraction (XRD). This review critically examines the challenges of qualitatively and quantitatively evaluating additive content using these methods, while highlighting their strengths and limitations, and how combinations of techniques can be used synergistically to enhance capabilities. This review aims to provide foundational insights and a potential roadmap for researchers and engineers who are beginning to explore polymer additives.

Received 17th October 2025,  
Accepted 13th January 2026

DOI: 10.1039/d5lp00329f

rsc.li/rscaplpoly

## 1. Introduction

Polymer additives are indispensable components of plastic formulations, serving a critical role throughout the material life-cycle. They are essential for preserving material integrity under the thermal and mechanical stresses of melt processing, modulating functional properties such as elasticity, mechanical strength, and barrier resistance to meet specific application requirements, and extending operational lifespan through long-term environmental stabilization. By enabling this precise tuning of chemical and physical characteristics, addi-

tives have transformed polymers from simple commodities into highly engineered materials, driving the continuous advancement and diversification of plastic technologies.<sup>1–3</sup> The type and concentration of additives incorporated in polymer materials vary with application area, *e.g.*, automotive, smart devices, healthcare, energy storage, and food packaging. Additives encompass a diverse range of chemical structures, each serving specific functions. However, they can generally be categorized into three types: those that preserve the inherent properties of polymers during polymer synthesis and processing, those that prolong the lifespan of the plastic application, and those that modify the polymer's material properties, enabling use in some applications.<sup>4</sup> The first category includes additives that facilitate shaping of plastics and protect them from degradation caused by heat, oxidation, mechanical stress, or chemical exposure during processing. These additives help maintain the integrity of the polymer chains and

<sup>a</sup>Department of Chemical Engineering, Auburn University, Auburn, AL 36849, USA<sup>b</sup>College of Forestry, Wildlife and Environment, Auburn University, Auburn, AL 36849, USA<sup>c</sup>Department of Mechanical Engineering, Auburn University, Auburn, AL 36849, USA.  
E-mail: ewd0001@auburn.edu

**Table 1** Summary of common additive types, examples, and their function

Additive type	Examples	Function
Plasticizer	Phthalate esters: di(2-ethylhexyl) phthalate (DEHP), dibutyl phthalate (DBP), diisononyl phthalate (DINP), diisodecyl phthalate (DIDP), diphenyl phthalate (DPHP), dimethyl phthalate (DMP) Non-phthalate esters: dimethyl adipate (DMA), diethyl adipate (DEA), and tributyl citrate (TBC) <sup>8–11</sup>	Tailor polymer flexibility <sup>7,29</sup>
Antioxidants	Lactones, acrylated bis-phenols, hindered phenols, aromatic amines, organophosphorous compounds, diestearyl thiodipropionate (DSTDP) <sup>13–15</sup>	Provide long-term thermal stability <sup>13–15</sup>
Heat stabilizers	Calcium/zinc salts, organotin compounds <sup>15</sup>	Provide long-term thermal stability <sup>15</sup>
Slip additives	Fatty acid amides, especially primary, erucamide, oleamide <sup>16,17</sup>	Reduce friction at the polymer surface <sup>16,17</sup>
Processing aids	Amide waxes, hydrocarbon waxes, fatty acids, fatty alcohols, and esters, vinylidene fluoride, hexafluoropropylene <sup>18–20</sup>	Reduce friction between polymer chains <sup>18–20</sup>
Fire retardants	Halogenated phenols, diphenyl esters, cyclododecane, phosphates, phosphonic acid derivatives, hydroxides of aluminum and magnesium <sup>21–23</sup>	Suppress ignition and reduce flame spread <sup>21–23</sup>
UV stabilizers	Hindered amine light stabilizers (HALS), metal complexes such as nickel chelates, or avobenzones <sup>24–26</sup>	Protect against UV light <sup>24–26</sup>

preserve molecular weight. Typical examples in this group include plasticizers (PL), antioxidants (AO), heat stabilizers (HS), processing aids (PA), and slip additives (SA). Another category of additives is those that prolong the service life of plastic products during end-use applications. These include UV/light stabilizers (UVS), antimicrobials, and some antioxidants (AO). Such additives help preserve a polymer's molecular structure and maintain its performance over time, especially under challenging conditions like outdoor exposure, UV radiation, microbial attack, and electrostatic discharge. The third category of additives includes nucleating agents, clarifiers, surface modifiers, impact modifiers, pigments, optical brighteners, fillers, phosphorus-based modifiers, boron-based electrolytes, flame retardants (FR), and antifogging or antistatic agents. These additives modify the mechanical, thermal, electrical, and surface properties of the polymer, enabling its use in applications requiring a specific property set, for example, transparent PP jars or flame-retardant clothing. In most cases, these additives improve polymer properties without altering

their molecular weight or backbone structure. However, chain extenders, cross-linking, and branching agents react with the polymer chains, leading to significant changes in the polymer's molecular structure and mechanical behavior.<sup>4–6</sup>

Another broad classification of polymer additives is whether they are organic or inorganic. Organic additives are carbon-based compounds, while inorganic additives are composed of mineral or metallic elements. The choice between organic and inorganic additives depends on the intended application, required performance, and environmental or regulatory considerations. The following paragraphs review several common additive categories, their chemical structures, and functions.

Among the many additive categories, plasticizers (PL) are one of the most widely used, playing a role in tailoring polymer flexibility and processability. They work by increasing the free volume of the system, thus decreasing characteristic relaxation times of the material.<sup>7</sup> PL are usually grouped into two different classes: phthalate esters and non-phthalate

**Tanmay Rahman**

*Tanmay Rahman is a Ph.D. researcher in the Department of Chemical Engineering at Auburn University. His research focuses on multilayer food packaging recycling, developing strategies to recover and repurpose complex polymer structures, and investigating the processability of recycled polymers for circular economy applications. In addition, he explores the structure–property–process relationships of bio-derived nano-*

*materials, such as cellulose nanocrystals (CNC), for mass sensing applications to advance towards sustainability.*

**Daniel Meadows**

*Daniel Meadows is currently a research engineer at ReLogic Research. He obtained both his Ph.D. and B.S. in chemical engineering from Auburn University. During his Ph.D. work, he focused on polymer engineering leveraging analytical laboratory techniques like FTIR, Raman, rheology, and thermal analysis.*





Fig. 1 (A) A general chemical formula of phthalate ester plasticizer, and (B) the non-phthalate ester plasticizer (DMA).

esters (Table 1). Around 85% of all PLs used worldwide are phthalate esters. Chemical structures of phthalate and non-phthalate esters are shown in Fig. 1. Approximately 90% of PLs are used in the production of plasticized or flexible polyvinyl chloride (PVC) products. Smaller quantities of plasticizers are also incorporated into other polymer systems such as polyvinyl butyral, acrylic polymers, polyvinylidene chloride, nylon, polyolefins, polyurethanes, and certain fluoroplastics.<sup>8–11</sup> The global plasticizer market is a significant segment of the polymer additives market. Recent reports estimate the market at approximately \$17.0 billion in 2022, with projections indicating growth to \$22.5 billion annually by 2027.<sup>12</sup>

While plasticizers primarily enhance flexibility, maintaining the long-term stability of polymers requires the addition of antioxidants (AO) (Table 1), which inhibit oxidative degradation during processing and service life.<sup>13–15</sup> Some examples of commercial AO are shown in Fig. 2(A and B). The primary thermal degradation pathway for halogen-containing polymers such as polyvinyl chloride (PVC), polyvinylidene chloride (PVDC), and chlorinated polyethylene (PE) is dehydrochlorination, rather than oxidation, leading to HCl release, polyene and carbenium formation, and discoloration. Since AOs are

ineffective against this mechanism, heat stabilizers (HS) are used instead (Table 1). These compounds scavenge the released HCl and stabilize the formed defects. The chemical structure of a heat stabilizer is shown in Fig. 2(C). They function by neutralizing HCl, reacting with polyenes, and eliminating carbenium salts. Costabilizers like organic phosphites, epoxides, polyols, and  $\beta$ -diketones are also commonly used to enhance the performance of primary stabilizers by regenerating consumed stabilizers.<sup>15</sup> Together, these systems provide long-term thermal stability and extend the service life of PVC products under processing and end-use applications.

Beyond enhancing flexibility and maintaining stability, additives can also modify surface properties. For example, slip additives (SA) (Table 1) reduce friction between polymer films and equipment, aiding extrusion and packaging processes.<sup>16,17</sup> The chemical structure of a commonly used SA is shown in Fig. 3(A). It is advantageous for these additives to “bloom” to the surface, forming microcrystalline layers that lower friction.<sup>17</sup> Processing aids (PA) (Table 1) are additives that enhance the handling and melt processability of high-molecular-weight polymers. They mainly function during the melt stage and fall into two categories: lubricants and fluoropolymer-based additives. These



Ke Zhan

Ke Zhan received his PhD in Forestry from Auburn University in 2025 and his master's degree in Wood Science and Technology from Southwest Forestry University in 2021. His research focuses on utilizing forest-based feedstocks to develop sustainable polymer composites, aiming to address critical environmental challenges.



Harrish Kumar Senthil Kumar

Harrish Kumar Senthil Kumar is a 4th-year PhD candidate in the Chemical engineering department at Auburn University. His work specializes in the recycling/recovery and characterization of multilayered packaging plastics. In addition, he also works on the innovative use of 3D printing technologies to create reactive porous media, a key component in studying subsurface systems. Through this interdisciplinary approach, he aims to enhance the understanding of material behavior in both environmental and sustainable engineering contexts.





**Fig. 2** Antioxidants such as (A) Irganox 1010 (hindered phenols), (B) DPPD-*N,N'*-diphenyl-*p*-phenylenediamine (aromatic amines), and (C) an organotin heat stabilizer.

additives reduce melt viscosity, limit melt fracture, and minimize material sticking to metal surfaces. Internal lubricants help polymer chains slide past each other, improving flow.<sup>18–20</sup> The chemical structures of a lubricant and fluoropolymer-based additives are shown in Fig. 3(B and C).

In applications where fire safety is critical, flame retardants (FR) are incorporated to suppress ignition, reduce flame spread, and limit the release of heat and smoke during combustion. There are a wide variety of compounds used as FR (Table 1).<sup>21–23</sup> For polymers used in outdoor applications, the

absorption of sunlight, including ultraviolet (UV), visible, and infrared radiation, is unavoidable. This exposure eventually leads to the oxidative degradation of photosensitive molecules in the polymer. This weathering can result in yellowing, embrittlement, and other unwanted property changes in the material. To reduce the rate of degradation, UV stabilizers (UVS) (Table 1) are used.<sup>24–26</sup> The structures of common UVS (avobenzene and hindered amine light stabilizers (HALS), partial structure) are shown in Fig. 4. All HALS contain this partial structure as part of their overall chemistry.



**Marshall Smith**

*Marshall Smith is currently a PhD student in Dr Edward Davis's lab at Auburn University in the Materials Engineering Program. He is researching the dissolution of multilayer polymer structures and thermal degradation characteristics, mixed with gas chromatography and mass spectrometry. His research interests are polymer composites, 3D printing, and space-based materials.*



**Edward Davis**

*Edward W. Davis (Ph.D., University of Akron) is an Associate Professor of Materials Engineering at Auburn University. Following an 11-year career in the plastics industry at Shell Chemicals and EVALCA, his research now focuses on the environmental and biological applications of polymeric nanomaterials and polymer recycling. Dr Davis is also a dedicated STEM education researcher, specifically investigating how integrating global societal challenges into the curriculum can motivate engineering interest among high school students. His work bridges advanced polymer science with pedagogical strategies to promote engineering as a viable and impactful career.*



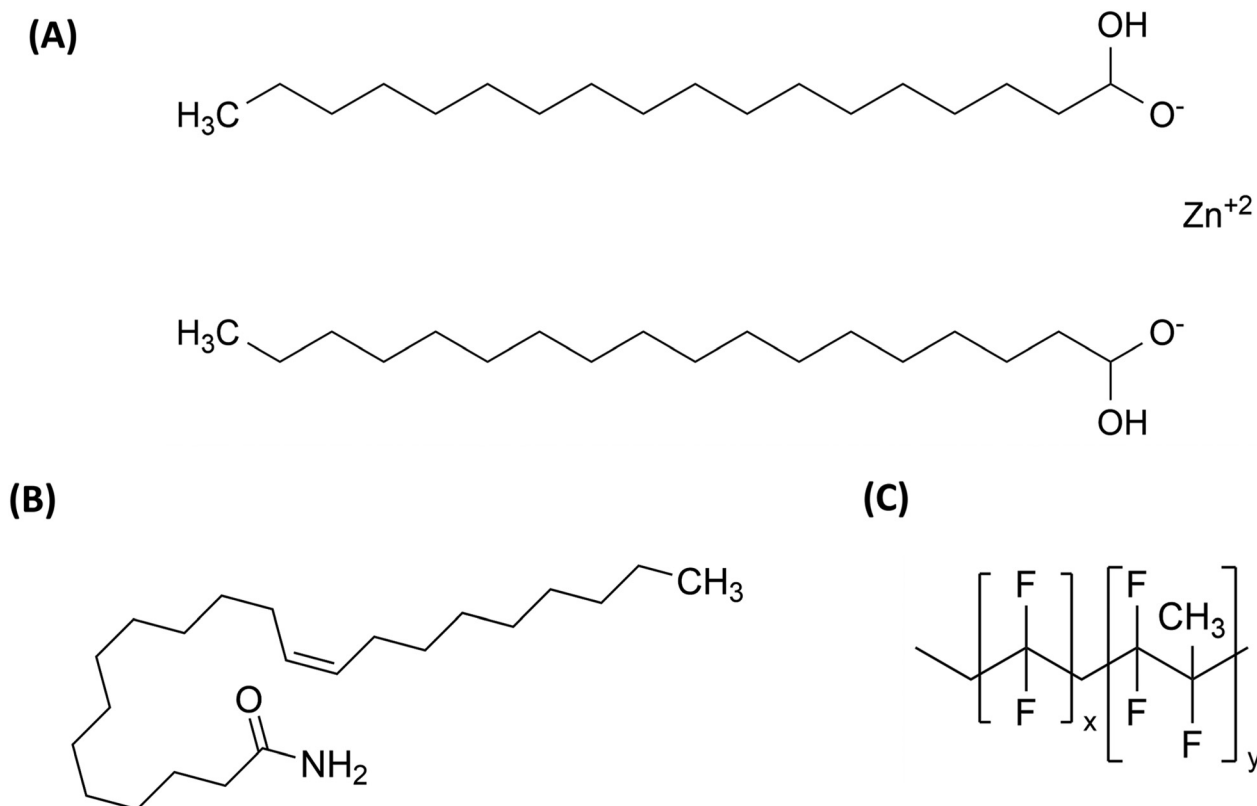


Fig. 3 Structure of (A) erucamide (a common slip additive), (B) metal soap (lubricant), and (C) vinylidene fluoride-hexafluoropropylene copolymers (fluoroelastomers).



Fig. 4 UV stabilizers: (A) partial structure of HALS, (B) avobenzene.

As the preceding discussion illustrates, the diversity and functional scope of additives within the polymer industry are extensive. Additive incorporation is rarely a singular event; instead, different additives may be added at various points in the polymer production and conversion process. In addition, understanding additive levels is essential for the valorization of reclaimed materials and for assessing the environmental impacts of microplastics. Thus, the necessity of detecting, identifying, and quantifying polymer additives spans the entire material lifecycle from synthesis to processing to end-of-life reclamation.

At the earliest stages, inhibitors may be introduced to the monomer to prevent premature polymerization, while post-

reactor operations such as solvent flushing or drying may require stabilization to protect the base resin. Following synthesis, the melt-processing and compounding stage represents the most intensive period for additive introduction. During extrusion, the polymer is subjected to high shear and thermal stress, necessitating the precise dosing of primary and secondary antioxidants. Functional masterbatches containing pigments, flame retardants, or UV stabilizers may be added to the melt. Determining additive concentrations in the compounded material is critical to ensuring it performs as intended. The last possibility of additive introduction before the polymer product is in use is during the conversion step, where the polymer is shaped into the final product by injection molding,



blow molding, film molding, thermoforming, casting, or a host of other specialized processes. During all these stages, additives should be uniformly dispersed within the polymer. Poor dispersion, side reactions, volatilization, or partial degradation can lead to defects such as discoloration, brittleness, loss of stability, or inconsistent mechanical properties. For this reason, quality control necessitates additive tracking at multiple points in the value chain. In addition, while the polymer product is in service, additives can leach or degrade over time, and understanding this behavior is an important aspect for ensuring the long-term performance of these products.

The analytical challenge intensifies during recycling and end-of-life processing. As plastics enter the circular economy, additive analysis becomes vital for 'technical traceability'. Recycled streams often contain unknown 'legacy additives', such as certain brominated flame retardants or heavy-metal stabilizers that were once standard but are now restricted by modern regulations (*e.g.*, REACH or RoHS).<sup>27</sup> Quantifying these additives is necessary to determine the safety and compatibility of the recyclate for high-value applications, such as food-contact packaging. Furthermore, because additives can migrate or leach over time, measuring their residual concentration is a key predictor of a material's remaining service life and mechanical viability after multiple heat histories.

Finally, the analytical scope has broadened to include the characterization of microplastics in environmental matrices. Additive profiles act as 'chemical fingerprints' that allow researchers to trace microplastic fragments back to their original industrial sources or applications (*e.g.*, heat stabilizers in glass-reinforced nylon engine components *versus* optical brighteners and softeners in nylon textile fibers). Understanding the additive concentration within microplastics is also critical for toxicological assessments, as these chemicals may desorb into the environment or bioaccumulate in the food chain.<sup>28</sup> Consequently, robust analytical protocols are required not only for quality control in manufacturing but as essential tools for environmental forensic analysis and the advancement of global plastic sustainability.

In polymer synthesis, compounding, and conversion, the chemical identities and loadings of both the polymer and its additives are typically well-defined. In contrast, the recycling stage often presents significant unknowns regarding additive chemistry, while environmental testing may lack certainty regarding the polymer matrix itself. Generally, researchers face four primary scenarios based on the degree of prior knowledge concerning the polymer, the additives, and their respective concentrations (Table 2). The amount of information known and thus the ability to rationally select analytical methods varies significantly between these scenarios, complicating additive analysis.

Despite advancements in analytical techniques, polymer additive analysis remains a critical challenge due to the typically low concentrations and complex interactions with the polymer matrix. In addition, while a plethora of methods is available, there is no single technique that can be applied to

**Table 2** Scenarios for polymer additive analysis

Polymer identity	Additive identity	Additive concentration	Typical context
Known	Known	Unknown	Polymer production, compounding, or converting operations Lab-produced samples for leaching, migration, or distribution studies where additive quantification is required
Known	Unknown	Unknown	Commercial products in which the formulation is proprietary, and the presence of additives is not disclosed Recycling operations where the broad class of polymer may be known, but the specific grade is not
Unknown	Unknown	Unknown	Common in microplastics and occasionally in the recycling stream. Materials may contain degraded additives
Unknown	Known	Known or unknown	A rare situation that can occur when a known additive marker is detected first, but the polymer identity remains unresolved

all additive chemistries. Each method applies only to a few additive chemistries and is often limited to a narrow concentration range.<sup>4</sup> As a result, detecting, identifying, and quantifying polymer additives is challenging, particularly when little to no information is available, such as in recycled materials and microplastic analysis.

To navigate these complexities, we propose a strategic analytical roadmap (Section 8) that matches specific techniques to these states of knowledge. While individual methods are reviewed in the following sections to establish their technical capabilities, the roadmap integrates these findings into a systematic framework for analyzing polymer additive systems.

Throughout this paper, the terms detection, identification, and quantification are used with precision. Detection refers to determining whether an additive is present in a sample (*i.e.*, what types (plasticizers/antioxidants) of additives are present). Identification refers to determining which specific additive is present (*i.e.*, which antioxidant is present). Quantification refers to measuring the amount of a particular additive present. These distinctions will be maintained consistently. The term "additive analysis" will refer to either detection, identification, quantification, or a combination of these activities.

The most common techniques for detecting, identifying, and quantifying polymer additives are listed in Table 3. The methods of additive analysis are broadly classified as spectroscopic, chromatographic, elemental, polymer property, and



**Table 3** Summary of the techniques and their applications to additive analysis found in the literature

Technique classification	Methods	Applicable additive class <sup>a</sup>	Sensitivity <sup>b</sup>
Spectroscopic	FTIR	PL, <sup>33</sup> HS, <sup>34</sup> SA, <sup>35</sup> PA, <sup>36</sup> IM, <sup>36</sup> FL <sup>36</sup>	Low
	Raman	PL <sup>37,38</sup>	Low
Chromatographic	NMR	AO, <sup>39</sup> SA, <sup>40</sup> P based modifier, <sup>41</sup> B and F based electrolyte <sup>42</sup>	High
	GC-single response detectors	PL, <sup>43</sup> AO, <sup>44</sup> UVS, <sup>45</sup> HS <sup>43</sup>	Low
	GC-spectral detectors	FR, <sup>46</sup> AO, <sup>45</sup> UVS, <sup>45</sup> OPA <sup>47</sup>	High
Elemental	HPLC	AO, <sup>48–51</sup> UVS, <sup>49,50</sup> PL <sup>50</sup>	High
	CHNS	N and S based additives <sup>52–54</sup>	High
	ICP	As, Bi, Cd, Co, Cu, Hg, Mn, Mo, Ni, Pb, Sb, Sr, Ti, V, Zn, B, P based IA <sup>55,56</sup>	High
Polymer property	SEM-EDS	FR, <sup>57,58</sup> IA, <sup>59</sup> FL <sup>60</sup>	Low
	TGA	FR, <sup>61</sup> FL, <sup>62</sup> IA <sup>52</sup>	Low
	DSC	CMB, <sup>63,64</sup> PL <sup>65</sup>	Low
	XRD	UVS, <sup>66</sup> PL <sup>67,68</sup>	Low
Evolved gas analysis	TGA-FTIR	AO, <sup>52</sup> PA <sup>52</sup>	Low
	TGA-MS	OPA <sup>69</sup>	High
	TGA-GC/MS	FL, <sup>70</sup> FR <sup>71</sup>	High

<sup>a</sup> AO = antioxidants, CMB = compatibilizers, FL = fillers, FR = flame retardants, HS = heat stabilizers, IM = impact modifiers, IA = inorganic additives, OPA = organic polymer additives PL = plasticizers, PA = processing aids, SA = slip additives, UVS = light stabilizers. <sup>b</sup> Techniques capable of detecting additives only at concentrations above ~100 ppm are considered to have low sensitivity. By contrast, methods that can detect additives at concentrations below ~100 ppm are regarded as high sensitivity.<sup>72</sup> This cutoff is not an absolute standard but provides a benchmark for comparing the detection capabilities of different techniques.

evolved gas analysis methods. Spectroscopic methods can identify typical molecular structures, which are then correlated to additive structures and used to deduce which additives are present in the material. Spectroscopic methods such as Fourier transform infrared (FTIR) and Raman spectroscopy provide molecular insights.<sup>30</sup> Nuclear magnetic resonance (NMR) spectroscopy further enhances structural understanding by revealing the chemical environment.<sup>31</sup> In all cases, these methods have low sensitivity and may not detect additives in low concentrations. To obtain detailed chemical structural information, chromatographic techniques are employed to separate and characterize additives from one another, from the polymer matrix, and from polymer degradation products, which may be present. Chromatographic methods separate the sample, typically by size, reducing the polymer's confounding effects on the additive's measurement. As a result, these methods vary in their ability to detect and identify additive classes. Chromatographic techniques for additive analysis can be broadly divided into gas chromatography and liquid chromatography. Gas chromatography (GC) with single response detectors such as flame ionization detectors (FID), flame photometric detectors (FPD), and nitrogen-phosphorus detectors (NPD) allows quantification of compound classes by detecting general signal intensities. Coupling GC with detectors such as mass spectrometry (MS), atomic emission detection (AED), or FTIR spectroscopy allows for more detailed structural and elemental analysis. Overlapping degradation products from both polymer and additives can complicate interpretation.<sup>32</sup> In comparison, elemental techniques such as, inductively coupled plasma (ICP), carbon/hydrogen/nitrogen/sulfur (CHNS) analysis, and energy dispersive X-ray spectroscopy (EDS) have relatively high sensitivity, but do not

provide information regarding the chemical structure. Elemental methods, as the name suggests, identify the elements present. Comparing these to additive chemistry can be used to deduce the type of additive and is particularly useful in identifying inorganic additives. While elemental methods reveal the elements present in additives, they often provide limited insight into the full molecular structure. In contrast to other approaches, polymer property-based methods assess changes in the bulk polymer's behavior to infer additive presence. As a result, they are useful in detecting if a particular type of additive is present, for example, a plasticizer, but not as helpful in identifying the specific chemistry of the additive. Thermal analysis, such as thermogravimetric analysis (TGA) and differential scanning calorimetry (DSC), can be used to infer the presence of additives by analyzing thermal decomposition profiles or phase changes in the polymer. Structural analysis, such as X-ray diffraction (XRD), can be used to infer the presence of additives by evaluating changes in crystalline content and structure. However, these methods have low quantitative sensitivity and do not elucidate the chemistry of the additives. Although they may indicate that an additive, such as a nucleating agent or a flame retardant, is present, they cannot identify the type or quantify the concentration. When both additive analysis and assessment of their thermal behavior are required, evolved gas analysis (EGA) provides a valuable bridge, coupling controlled thermal decomposition with a range of detection systems. Common EGA approaches include TGA-MS, which links mass loss to molecular ion information; TGA-FTIR, which identifies evolved gases based on their infrared spectra; and TGA-GC/MS, which separates volatile products before detailed mass spectrometric identification.



This review assesses these techniques and establishes basic governing principles for their application to additive analysis. The discussion is structured into five main categories: spectroscopic, chromatographic, elemental, polymer property, and evolved gas analysis methods. Each section begins with a general overview of the category, followed by a detailed discussion of the individual techniques within it. The working principles, capabilities, and limitations are discussed. Recent literature applying each method to additive analysis is then reviewed. This paper also introduces a proposed roadmap for improving additive analysis by strategically combining multiple methods. By providing a detailed assessment of each method and a proposed roadmap for analysis, this paper lays a foundation for future research. It enables researchers to conduct more accurate, robust analysis of polymer additives.

## 2. Methodology for selecting papers to review

The literature reviewed in this article was selected to provide a comprehensive and balanced overview of analytical techniques used for polymer additive detection, identification, and quantification. Priority was given to recent publications (within the past 10–15 years) to capture the latest methodological developments, applications, and challenges reported in the field. These studies were sourced from peer-reviewed journals and reputable scientific databases, ensuring coverage of contemporary advances in spectroscopic, chromatographic, thermal, and elemental analysis methods. At the same time, it was recognized that several chromatographic and hyphenated techniques have a long history of application to polymer additive analysis. Consequently, earlier landmark papers were also included, where they provided essential background, introduced techniques that remain widely used today, or established reference points for later methodological development.

## 3. Spectroscopic techniques

Spectroscopic techniques such as Fourier transformed infrared (FTIR) spectroscopy, Raman spectroscopy, and nuclear magnetic resonance (NMR) spectroscopy are widely employed for detecting and characterizing polymer additives. These techniques provide complementary insights into the molecular composition, structural arrangement, and chemical interactions of additives within polymer matrices. Both FTIR and Raman spectroscopy use vibrational transitions to identify molecules. FTIR spectroscopy detects changes in a molecule's dipole moment, whereas Raman spectroscopy measures changes in its polarizability, the molecule's ability to develop an induced dipole. Together, these two techniques can be used to map out the molecule's vibrational fingerprint. NMR spectroscopy probes the magnetic properties of atomic nuclei; the resonance frequency of these nuclei's spins is affected by the local chemical environment (*i.e.*, nearest neighbor atoms).

Thus, NMR spectroscopy can reveal information related to molecular configuration.

### 3.1. FTIR spectroscopy for polymer additive analysis

**3.1.1. Fundamentals and limitations.** FTIR spectroscopy is a routine characterization technique found in many laboratories. Simplified schematics of the two most common types of FTIRs: attenuated total reflectance (ATR) and transmission, are provided in Fig. 5(A). In FTIR spectroscopy, infrared radiation from the source is split into two beams by a beam splitter. One beam is directed to a stationary mirror, while the other is directed to a moving mirror, which moves back and forth during the measurement. The two beams are then reflected by their respective mirrors and recombined at the beam splitter, where they interfere with each other. The mirror's motion is critical because it modulates the interference, enabling the acquisition of a broad spectrum of IR wavelengths. For ATR mode FTIR (ATR-FTIR) spectroscopy, this beam then passes through a crystal in such a way that the beam is reflected at the surface between the adjacent medium and the crystal. An evanescent wave is formed, which extends into the adjacent medium and penetrates the sample surface. The penetration depth is usually on the order of one micron.<sup>73</sup> The reflected beam eventually reaches the detector, producing an interferogram, a plot of mirror position *versus* IR intensity. It is important to note that ATR-FTIR spectroscopy is a surface measurement and not a bulk probe of the material. Thus, because additives are often incorporated and distributed irregularly within plastics, many measurements at different locations of the sample should be taken. However, ATR-FTIR spectroscopy is an excellent technique for analyzing additives that may have bloomed from the bulk polymer. In contrast, for transmission-FTIR spectroscopy, the recombined IR beam is directed through the bulk of the sample, which is typically prepared as a thin film or a pressed KBr pellet. KBr is used to dilute the sample so that the absorption is not too strong. The beam travels entirely through the sample, and the frequencies absorbed correspond to specific molecular vibrations within the material. Because the beam traverses the full thickness, transmission-FTIR spectroscopy provides information about the entire volume of the material rather than just the surface.<sup>74</sup> When IR light interacts with a molecule, specific frequencies are absorbed corresponding to the vibrational frequencies of the bonds (stretching, twisting, rocking, scissoring) within the molecule, as shown in Fig. 5(B). The resulting interferogram is converted using the Fourier Transform to generate FTIR spectra. Each functional group absorbs light at a characteristic frequency. Thus, the absorbance spectrum of a material depends on the functional groups present and, conversely, can be used to identify them.

Typically, a molecule is "IR active" if there is a change in its dipole moment during its vibration, as this vibration produces its own oscillating electric field, which interacts with the oscillating electric field of the incoming IR. If the frequencies of the incoming IR and molecular vibration match, the incoming IR wave is absorbed. While FTIR spectroscopy is a powerful





**Fig. 5** (A) Two typical modes of FTIR spectroscopy: ATR, and transmission; (B) IR interacting with different vibrational modes that create a change in dipole moment of the bonds and result in an interferogram and finally a FTIR spectra; (C) deconvolution of a FTIR spectra within a wavenumber range b to c to identify four peaks at different positions.

characterization tool for identifying functional groups and additives in polymers, several factors hinder its usefulness in detection, identification, and quantification. In general, chemical applications of group theory suggest that symmetric vibrations are not usually detected by IR spectroscopy, limiting the detection of molecules that do not exhibit a change in dipole moment during vibration.<sup>75,76</sup> FTIR spectra often exhibit broad or merged peaks that may contain multiple vibrational modes from different chemical groups within the polymer matrix and the additives. The deconvolution of an FTIR spectrum within a wavenumber range is shown in Fig. 5 (C). The deconvolution of these peaks is quite challenging and requires access to reference databases. Prior knowledge of the sample composition enables the selection of appropriate reference spectra or databases for accurate peak assignment.

For a known polymer with unknown additives, broader, more comprehensive spectral libraries must be employed, leading to greater uncertainty in signal interpretation. Multivariate curve resolution (MCR) in FTIR spectroscopy can be useful in such cases. MCR refers to a technique used to decompose complex spectral data into individual component spectra and their corresponding concentrations without

knowing the exact identity or number of components in advance. The identification of trace components in the bulk polymer becomes increasingly challenging when more than one additive is present, considering the quite poor detection limit of FTIR spectroscopy (~100 ppm) compared to other techniques such as mass spectroscopy.<sup>77,78</sup> Again, the quantification of additives with FTIR spectroscopy relies on the fact that the absorbance of a specific IR band is proportional to the concentration of the species of interest and the path length of the interacting IR beam. In contrast to transmission-FTIR spectroscopy (where the path length is fixed and known), the path length in ATR-FTIR spectroscopy depends on the refractive indices of the sample and the crystal, the penetration depth of the evanescent wave, and the quality of contact between the sample and the crystal. These factors make ATR-FTIR spectroscopy less suitable for direct absolute quantification. However, relative quantification remains highly effective in ATR-FTIR spectroscopy, which focuses on comparing changes in peak intensities between samples. In this approach, the analysis determines how much more or less an additive is present relative to a reference or control sample. This is commonly achieved using internal standards and cali-



bration curves that relate peak ratios to known concentration differences.

FTIR spectroscopy can identify classes of additives such as heat stabilizers, slip additives, and plasticizers in various polymers, but it is not useful when certain fillers are present. Inorganic pigments like titanium dioxide or carbon black can strongly absorb or scatter infrared light, distorting or obscuring the signals of other substances. Some inorganic fillers, like calcium carbonate may produce identifiable peaks, but their presence in high concentrations or in combination with pigments can still lead to overlapping signals or baseline distortions. In these cases, other analytical techniques such as thermogravimetric analysis (TGA), differential scanning calorimetry (DSC), and X-ray diffraction (XRD), or other coupled techniques can be used to provide additional insight. While there are drawbacks to using FTIR spectroscopy for additive detection in polymers, there are still some benefits. For instance, FTIR spectroscopy is a common instrument found in many analytical labs, making it widely accessible. Likewise, it is a simple, non-destructive technique that can provide rapid spectra for bulk samples. When coupled with other techniques such as TGA, significantly more information about trace components can be obtained. Moreover, subtractive FTIR spectroscopy can be used to detect subtle spectral changes between a reference sample and one containing additives or trace components of interest.<sup>79</sup>

**3.1.2. Recent advances and current trends.** Bernard *et al.* utilized FTIR spectroscopy to screen plasticizers present in commercial medical devices composed of polyvinyl alcohol (PVC).<sup>33</sup> Plasticizers can leach into solutions administered to patients, potentially leading to direct exposure. Monitoring how the additive content in medical-grade polymers changes over time is crucial to understanding additive leaching. They found that ATR-FTIR spectroscopy was able to identify plasticizers such as acetyl tributyl citrate (ATBC), di(2-ethylhexyl) terephthalate (DEHT), di(2-ethylhexyl) adipate (DEHA), diisononyl phthalate (DINP), diisononyl cyclohexane-1,2-dicarboxylate (DINCH), tris(2-ethylhexyl) trimellitate (TOTM), and di(2-ethylhexyl) phthalate (DEHP) in medical devices.<sup>33</sup> Their work provides a guide for the use of FTIR spectroscopy, amongst other techniques, for the identification of plasticizers, specifically in medical devices. This suggests that rapid, routine screening of medical devices could be performed using FTIR spectroscopy to monitor additive migration in these systems.

Similarly, PVCs used as films and gaskets for bottle corks contain heat stabilizers such as Irgastab 17 MOK (dioctyl tin bis(2-ethylhexylthioglycolate)) that can migrate to food, potentially causing toxicological effects. Zeddard *et al.* studied this migration effect by adding 4.5 wt% of this heat stabilizer to PVC during solution casting in tetrahydrofuran, followed by drying to produce PVC films with additives to simulate a typical formulation.<sup>34</sup> The prepared PVC films were exposed to fatty food simulants (96% ethanol and hexane). Transmission-FTIR spectroscopy analysis of the PVC film revealed a decrease in the carbonyl absorption band at 1732 cm<sup>-1</sup> over time, indicating the migration of Irgastab 17 MOK out of the film. The

extent of this migration was quantified by calculating the ratio of the area under the carbonyl peak at 1732 cm<sup>-1</sup> to the area under a stable CH<sub>2</sub> reference peak at 1432 cm<sup>-1</sup> in the PVC matrix.<sup>34</sup> Agustina *et al.* used ATR-FTIR spectroscopy to identify and quantify slip additives such as erucamide as part of an evaluation of the effects of antiblock as migration control of the slip additive.<sup>35</sup> For this, erucamide and anti-blocks (including talc, silica mineral, and synthetic silica) were blended with a low-density polyethylene (LDPE) carrier resin to achieve a final concentration of 1500 ppm erucamide. To characterize erucamide migration to the film surface, the amide absorption peak in the 3200–3400 cm<sup>-1</sup> range, specifically at 3407 cm<sup>-1</sup>, was measured using FTIR spectroscopy over time. The concentration of the additive on the surface was determined by comparing the area under the absorbance curve at 3407 cm<sup>-1</sup> to that of an erucamide standard.<sup>35</sup> Both of these studies were effective at monitoring the migration of known additives within known polymer matrices. In contrast, Cuthbertson *et al.* explored using ATR-FTIR spectroscopy to detect unknown additives in three types of commercial ethylene vinyl acetates (EVA).<sup>52</sup> They noted the presence of C–Cl deformation modes in the 550–850 cm<sup>-1</sup> region, which implied the possibility of chloride-based additives; however, FTIR spectroscopy alone could not identify or quantify the specific additives.<sup>52</sup>

While these studies suggest that FTIR spectroscopy can be useful for identifying known additives in known polymers, identifying unknown additives remains challenging and requires FTIR spectroscopy coupled with peak deconvolution. Li *et al.* used an MCR on ATR-FTIR spectroscopy to identify unknown additives in low concentrations in two unknown elastomeric polymer materials.<sup>36</sup> The additives included zinc stearate (processing aids), trans-polysoprene (TPI) (impact modifier), and fillers like calcium carbonate (CaCO<sub>3</sub>) and talc. The authors successfully applied their MCR strategy, using reference spectra, to elucidate the components in their samples, thereby enabling the identification of the additives.<sup>36</sup> However, this study did not establish a quantitative method, suggesting that quantifying additives in polymers remains difficult, even when using advanced FTIR spectroscopy analysis.

Overall, the literature demonstrates that while FTIR spectroscopy is highly effective for monitoring migration in well-defined systems where characteristic absorption bands are known, its utility is significantly compromised in commercial materials with unknown additive packages. In complex formulations, spectral overlap and matrix interference often preclude confident identification through standard library matching. Although the integration of multivariate strategies, such as MCR, has advanced the qualitative identification of unknown additives, the literature indicates that achieving robust quantification remains a significant challenge due to the lack of standardized, matrix-independent methodologies.

### 3.2. Raman spectroscopy for polymer additive analysis

**3.2.1. Fundamentals and limitations.** Like IR spectroscopy, Raman spectroscopy provides information about a sample's



fundamental chemistry. As previously mentioned for the case of FTIR spectroscopy, a change in dipole moments gives rise to a molecule's IR activity. However, there is no IR activity for diatomic molecules such as  $O_2$  or molecules with completely symmetric vibrations from a center of symmetry (such as the symmetric stretch of  $CO_2$ ). In these cases, Raman spectroscopy can provide insight into the molecular structure. A vibration is Raman-active if it causes a change in the molecule's polarizability. A vibration can be both Raman and IR active if it induces a change in dipole moment and a change in polarizability, as in the case of the asymmetric stretch of O-H in water. In contrast to IR spectroscopy, which is an absorption technique, Raman spectroscopy is based on scattering. There are two primary types of light scattering: when the frequency of the scattered photon is the same as that of the incident photon, it is called Rayleigh scattering (elastic scattering); when the frequency differs, it is known as Raman scattering

(inelastic scattering). Stokes scattering and anti-Stokes scattering are two types of inelastic scattering processes. Stokes scattering results in a photon with a lower frequency than the incident photon, while anti-Stokes scattering results in a photon with a higher frequency than the incident photon, as shown in Fig. 6(A).<sup>80</sup> The relative change in wavenumber between the incident and scattered photon is known as the Raman shift. This shift depends on the type of bond doing the scattering and its surrounding chemical environment.<sup>81</sup> Thus, Raman spectroscopy can provide insight into both the scattering structures and their connections. A basic diagram of the Raman spectroscopy instrument is provided in Fig. 6(B).

In a typical Raman spectroscopy setup, a monochromatic laser in the near-IR or visible range serves as the excitation source. It is directed toward the sample using mirrors and a dichroic beam splitter. The beam splitter reflects the incoming laser light toward the sample while allowing the scattered light to pass through. When the laser light interacts with the sample, most of it is elastically scattered (Rayleigh scattering),

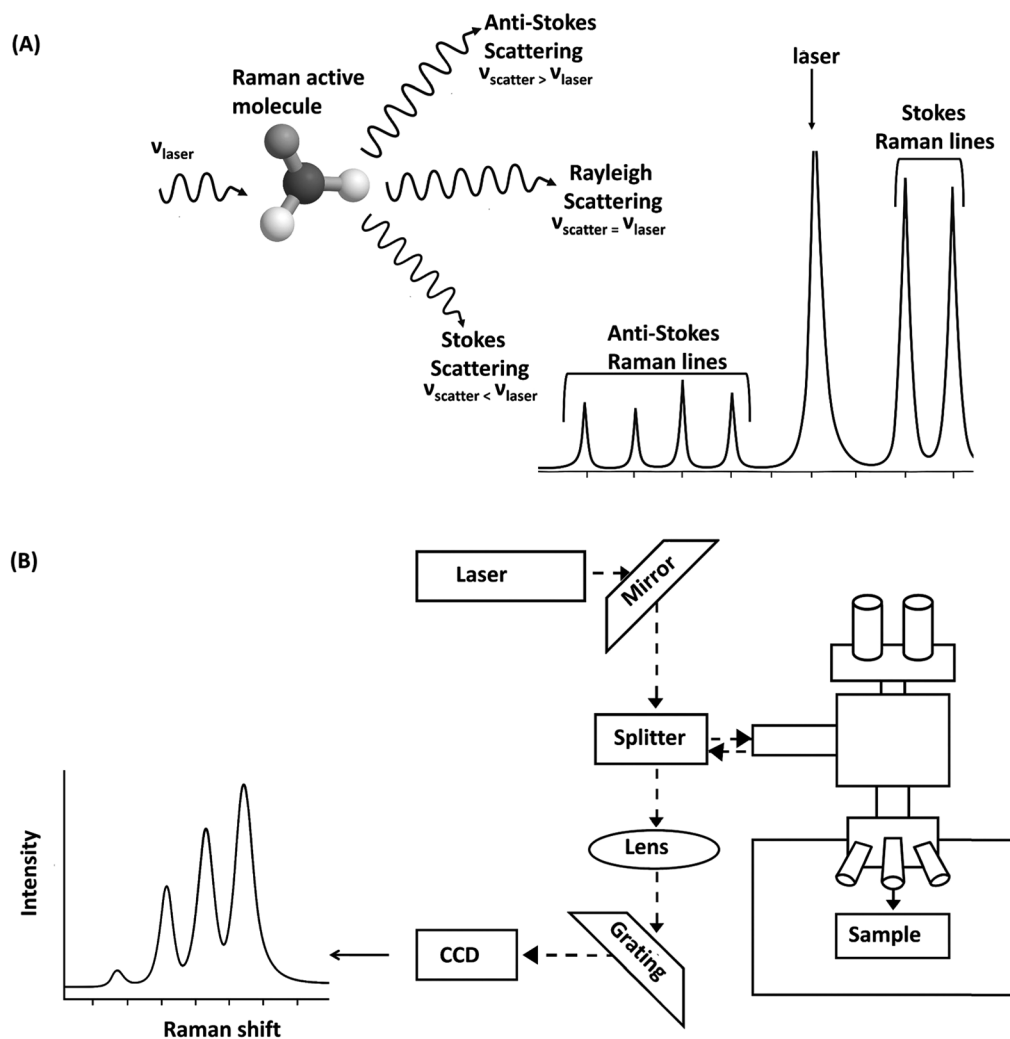


Fig. 6 (A) Interactions of a laser with a Raman active molecule resulting in Stokes and anti-Stokes Raman shifts, (B) schematic of a Raman spectrometer resulting in Raman spectra.



but a small fraction undergoes inelastic scattering (the Raman effect), where the scattered light shifts in energy due to molecular vibrations. The scattered light, containing both Rayleigh and Raman components, returns through the same optical path and passes through the beam splitter. Optical filters are then used to remove the strong Rayleigh component, allowing only the weak Raman-scattered light to proceed. This light is focused through a lens system and directed onto a diffraction grating, which disperses it based on wavelength. Finally, a CCD detector captures the dispersed spectrum, revealing the vibrational information of the molecules in the sample. The software can automatically compare the acquired spectrum with built-in spectral libraries to suggest possible compound identifications. However, in complex samples such as polymer blends or materials with multiple additives, peak overlap can make identification difficult. In these cases, running known standards (*i.e.*, pure additives within the same matrix) is essential for verifying peak assignments and improving accuracy.<sup>82</sup>

Compared to FTIR spectroscopy, Raman spectroscopy usually has less sensitivity. This can be attributed to the lower prevalence of inelastic scattered light compared to elastic scattered light, with Raman scattering occurring at an estimated ratio of about one in  $10^8$  scattered photons relative to Rayleigh scattering, thereby limiting the instrument's sensitivity.<sup>83</sup> Another key challenge is spectral overlap, where different additives may have similar or overlapping Raman bands, making it difficult to distinguish individual components, especially when they belong to the same chemical family (*e.g.*, various phthalate esters), making deconvolution protocols a critical necessity. Likewise, many commercial additives are found in low concentrations and may produce weak signals that are easily masked by the more intense bands of the polymer matrix or other additives.

**3.2.2. Recent advances and current trends.** Nørbygaard *et al.* used Raman spectroscopy to detect the presence of the phthalate ester di(2-ethylhexyl) phthalate (DEHP) plasticizer in different PVC consumer products by comparing their peaks with those of pure DEHP spectra that had characteristic peaks at 652, 1040, 1450, 1580, 1600, and 1726  $\text{cm}^{-1}$ .<sup>37</sup> They also discussed how calibration curves could be used to quantify the additive. However, they did not report a measured concentration and noted that it would be necessary to account for tertiary constituents (*e.g.*, filler materials) in the sample for quantitative accuracy.<sup>37</sup> Follow-up work by Berg and Otero sought to detect the presence of adipic acid di-esters plasticizers in commercial flexible PVC products using Raman spectroscopy by comparing the spectra with spectra of a range of adipate ester (AE) plasticizers in pure form.<sup>38</sup> However, they reported that identification of aliphatic esters using Raman spectroscopy is challenging, as their characteristic ester group bands, particularly those involving the carbonyl stretch, are not unique. Similar bands could appear in other aliphatic di-carboxylic esters and various carbonyl-containing compounds, such as those around 1734  $\text{cm}^{-1}$ . These spectral overlaps made it difficult to identify the exact type of esters present, especially in mixed samples. Additionally, they reported that AE signals

are generally weak compared to the strong Raman response of PVC, further limiting the ability to identify and quantify specific esters accurately.<sup>38</sup> An interesting study was conducted on plastic cast sculptures, in which the authors used a portable Raman spectrometer to determine composition.<sup>84</sup> Raman spectroscopy not only detected the plastic as PVC but also showed that the PVC contained phthalate plasticizers. Despite these examples, there is limited literature on the use of Raman spectroscopy for plastic additive analysis. Hummel suggested that this is due to several factors, which include:<sup>85</sup>

- Poor scattering and high fluorescence of certain materials
- Questionable reproducibility of spectra with similar instrumentation
- Lack of libraries or databases for additives

High fluorescence in Raman spectroscopy is often due to a polymer's low melting point or excessive laser energy, which can ablate the sample. Both issues cause interference with the measurement by creating broad bands of noise in the spectrum.

While Raman spectroscopy effectively identifies specific plasticizers within PVC matrices, its utility for broader additive analysis is restricted. This limitation stems from the inherently low Raman scattering cross-sections of many additives, which are frequently obscured by the dominant polymer signal. Furthermore, persistent challenges, including intense fluorescence, inconsistent spectral reproducibility, and a deficit of standardized reference libraries, hinder its adoption for universal application. Expanding these databases through quantitative material studies represents a critical and promising frontier for future research.

### 3.3. NMR for polymer additive analysis

**3.3.1. Fundamentals and limitations.** NMR spectroscopy is a powerful non-destructive technique where nuclei with magnetic moments interact with radiofrequency radiation. This method is primarily used for the quantification and characterization of small organic molecules and macromolecules and is widely used in chemistry, biology, food science, and pharmaceutical quality analysis. NMR spectroscopy operates on the principle that atomic nuclei with a net spin (like  $^1\text{H}$ ,  $^{13}\text{C}$ ,  $^{19}\text{F}$ ,  $^{31}\text{P}$ , *etc.*) interact with an external magnetic field and radiofrequency (RF) energy. When a sample is placed in a magnetic field (low or high), the nuclei align according to the field's direction. Applying a strong RF pulse excites the nuclei, causing them to absorb energy and flip their spins. The specific frequencies at which this absorption occurs depend on the chemical environment surrounding the nuclei. After the RF pulse ends, the nuclei tend to return from the excited state to the ground state, releasing a secondary RF pulse that can be detected. This secondary RF pulse is called the free induction decay (FID) of the applied RF pulse. The detected RF waves are converted to a spectrum for interpretation of the sample under study. The absorption of RF is based on the chemical environment surrounding the nuclei and can thus be used to differentiate atoms with different environments within



the same sample, for example, the proton NMR spectrum of 2-butanone would show three separate sets of peaks corresponding to the hydrogens at the terminal methyl group, the methyl group adjacent to the carbonyl, and the methylene group, thus demonstrating presence of these groups in the sample. Formally, the peaks in an NMR spectrum correspond to the resonance frequencies of specific nuclei in a magnetic field. These peaks are derived from the signals emitted as nuclei relax following an RF pulse. To ensure consistency, the frequency of each signal is referenced to a standard, typically tetramethylsilane (TMS). This difference in frequency, known as the chemical shift, is reported in field-independent units of parts per million (ppm). The shifts are either termed as downfield (signals at higher ppm) or upfield (signals at lower ppm). Downfield shifts are attributed to nuclei experiencing effects from nearby electronegative atoms or groups. Upfield shifts are attributed to the nuclei experiencing effects by surrounding electron-donating groups or the absence of nearby electronegative groups.<sup>86–90</sup> The resolution of the spectra varies based on the strength of the magnetic field used for analysis. Low field NMR spectroscopy has advantages such as the ability to use regular solvents, and less maintenance, but has lower sensitivity. High-field NMR spectroscopy offers several advantages, including higher sensitivity and the ability to perform advanced techniques with lower SNR (signal to noise ratio), thereby enhancing the resolution of the spectrum and improving quantification.<sup>91–93</sup> NMR spectroscopy typically has detection limits in the micromolar range.

A simplified diagram of NMR spectroscopy is shown in Fig. 7. Quantification can be performed by analyzing the inte-

grals of the peaks (areas under the peaks), which are proportional to the number of nuclei that contribute to each signal. The known peak's integral value is normalized (usually an internal standard) and is used to determine the relative ratios of the nuclei contributing to the peak.

One key challenge with NMR spectroscopy is its sensitivity for very dilute samples (*e.g.*, lower concentrations of the additives in the solution) or those with low natural abundance of NMR-active nuclei, leading to low resolution. Advanced NMR spectroscopy methods address these limitations in two main ways. First, correlation-based techniques such as two-dimensional (2D) NMR spectroscopy that correlate two NMR spectra, either of the same or different nuclei. This 2D NMR spectroscopy enables detailed structural analysis of molecules compared to 1D NMR spectroscopy. There are many 2D NMR spectra analysis techniques, such as proton–proton correlation spectroscopy (COSY), nuclear overhauser enhancement spectroscopy (NOESY), and heteronuclear single quantum correlation (HSQC), among others. However, while these methods improve resolution, they do not substantially overcome the fundamental sensitivity limitation and typically require longer acquisition times compared to 1D NMR spectroscopy. The hardware-based strategies, such as cryoprobes, dynamic nuclear polarization (DNP), and higher-field magnets, directly enhance sensitivity by increasing signal-to-noise ratios, making them more effective for low-concentration samples.<sup>94</sup>

**3.3.2. Recent advances and current trends.** Meadows *et al.* have used advanced NMR spectroscopy techniques such as DEPT <sup>13</sup>C NMR, HMQC, and COSY NMR spectroscopy techniques to detect the presence of lactones in EVOH and their



Fig. 7 A simplified diagram of NMR spectrometer, showing the magnet, RF transmitter, detector, and the resulting spectra plotted as chemical shift from downfield to upfield.



thermo-oxidative degradation, demonstrating the power of NMR spectroscopy for detecting trace components.<sup>95</sup> The study by Ehret-Henry *et al.* investigated the use of proton NMR spectroscopy to detect and identify polymer additives in polyolefin materials with unknown additive formulations.<sup>39</sup> Six samples were examined, including three polypropylene films from the food industry and three granule samples (one PP homopolymer and two PP/PE copolymers) from a plastics manufacturer, none of which had disclosed additive information. The NMR spectroscopy analysis successfully revealed the presence of several antioxidants-Irganox 1010, Irganox 1076, Irganox 1330, and Irgafos 168 as well as erucamide slip additives. These findings demonstrate NMR spectroscopy's ability to detect antioxidants and slip additives directly in complex polymer matrices without prior knowledge of the formulation. The work highlights the potential of NMR spectroscopy as a powerful tool for additive monitoring and safety control in food packaging materials. However, they suggested that combining NMR analysis with other techniques, such as GC-MS, is required for precise quantification.<sup>39</sup> Coelho *et al.* reported the preparation of polypropylene homopolymer composites containing 1–5 wt% of slip additives such as *N*-isopropyl stearamide and *N,N*-diisopropyl stearamide *via* extrusion.<sup>40</sup> The authors employed carbon and proton NMR spectroscopy to identify and differentiate the additives within the polymer matrix. In the case of *N*-isopropyl stearamide, the proton NMR spectrum clearly showed a singlet at 3.66 ppm corresponding to the N–H proton, confirming that the amide nitrogen retained one hydrogen. In contrast, *N,N*-diisopropyl stearamide lacked this N–H signal because both substituents on the nitrogen are isopropyl groups, rendering the amide tertiary. Additional spectral differences, such as the isopropyl methine multiplet at 3.94 ppm and shifts in carbonyl-adjacent methylene signals, reinforced the assignments.<sup>40</sup>

Zygadło-Monikowska *et al.* synthesized difluoroalkoxyboranes and trialkoxyboranes additives and identified their structures using boron and fluorine NMR spectroscopy before adding them to solid polymeric electrolytes comprising PEO as polymer matrix and 10 mol% of lithium salt.<sup>42</sup> In this case of the difluoro derivatives, the fluorine NMR spectrum showed signals around 58 ppm in chloroform and a characteristic quartet near –150 ppm in acetonitrile, indicating fluorine atoms directly bonded to boron. In contrast, the boron NMR spectra of these compounds gave signals at low chemical shifts (0–6 ppm), consistent with difluoroborane species. In contrast, the trialkoxyboranes displayed no fluorine resonance but gave boron NMR signals much further downfield, at about 18 ppm in chloroform and 23 ppm in acetonitrile, characteristic of fully alkoxylated boron centers. Together, these differences in boron and fluorine chemical shifts enabled clear identification of the di- and tri-substituted boron compounds.<sup>42</sup> These studies demonstrate that NMR spectroscopy is a reliable tool for distinguishing structurally similar additives in polymers.

Miknis *et al.* studied polyphosphoric acid (PPA) as a modifier in bitumen by preparing samples containing 1.5 wt% PPA.<sup>41</sup> Phosphorous NMR spectra of the blended material

showed resonances for orthophosphoric acid as well as for middle and end groups of phosphate chains, confirming the initial presence of polyphosphoric structures. At 135 °C, the chain group signal diminished, and the orthophosphoric acid resonance became dominant, indicating that PPA gradually reverted to its monomeric form.<sup>41</sup> This study suggests that phosphorus NMR spectroscopy provides a direct and sensitive means of tracking the chemical environment of phosphorus atoms, making it crucial for identifying structural transformations and monitoring additive stability for phosphorus-containing additives.

NMR spectroscopy is a definitive tool for the structural identification of additives, yet its application to polymer matrices involves significant practical constraints. The literature highlights that while NMR spectroscopy provides unmatched chemical specificity, its utility for additive analysis is often limited by poor sensitivity and the broadening of signals caused by the polymer environment. These challenges, combined with the requirement for specialized instrumentation and lengthy acquisition times, have prevented NMR spectroscopy from becoming a primary tool for rapid additive screening. Consequently, recent studies suggest that NMR spectroscopy is most effective when used as a complementary technique for the structural confirmation of unknown additives rather than a standalone method for high-throughput quantification.

In summary, spectroscopic techniques offer a spectrum of capabilities, ranging from high-throughput screening with FTIR spectroscopy to definitive structural confirmation with NMR spectroscopy. While each provides critical data, their effectiveness is often mediated by the complexity of the polymer matrix. These tools are thus positioned within the proposed roadmap (Section 8) as either primary filters or verification steps, depending on the initial state of knowledge regarding the sample.

## 4. Chromatographic techniques

Chromatographic techniques are essential tools for detecting and identifying polymer additives due to their ability to separate complex mixtures and resolve additive signals from those of the polymer matrix. Broadly, chromatographic techniques fall into two categories: gas chromatography (GC) for volatile or thermally stable compounds, and high-performance liquid chromatography (HPLC) for non-volatile or thermally sensitive species. GC, when paired with single-response detectors such as the flame ionization detector (FID), flame photometric detector (FPD), or nitrogen phosphorus detector (NPD), enables quantitative determination of specific classes of organic additives based on combustion products. Its capability can be further enhanced by pairing GC with spectral detectors – such as mass spectrometry (GC-MS), Fourier transform infrared spectroscopy (GC-FTIR), or atomic emission detection (GC-AED), which combine chromatographic separation with molecular, functional group, or elemental composition analysis. These systems overcome the limited chemical specificity of single-response detectors. For additives embedded within



the polymer, pyrolysis can be employed to thermally decompose the matrix and release volatile fragments for GC analysis, making it suitable for antioxidants, plasticizers, and stabilizers that survive or form identifiable products upon heating. In contrast, HPLC separates additives in the liquid phase based on their solubility and interactions with the stationary phase, allowing high-sensitivity detection—often with UV-Vis, fluorescence, or MS for compounds such as UV stabilizers, flame retardants, and processing aids without subjecting them to thermal stress. Together, GC and HPLC provide complementary pathways for detecting and quantifying a wide range of polymer additives according to their volatility, stability, and chemical nature.

#### 4.1. Gas chromatography with single-response detectors for polymer additive analysis

**4.1.1. Fundamentals and limitations.** In gas chromatography (GC), the separation of molecules is primarily based on two key properties: volatility and polarity. The process involves two phases: a mobile phase, typically an inert gas like helium (He), and a stationary phase located inside a column. The mobile phase carries the molecules through the column, where they interact with the stationary phase. As the molecules pass through, their varying polarities and molecular weights cause them to travel at different speeds, allowing separation and subsequent detection (FID, FPD, NPD). Each molecule or analyte has a specific residence time. Thus, two analytes that produce the same detector response can be identified individually based on their residence times in the column. The stationary phase can be either solid or liquid, and the columns used in gas chromatography may be packed-bed or capillary columns. This method is particularly useful for separating and analyzing organic molecules. Understanding the relationship between the mobile and stationary phases, the properties of the molecules being analyzed, and the mechanism of separation is essential to the successful application of gas chromatography. The sample can be solid, liquid, or gas. However, the molecules must be in the gas phase, which is usually achieved by pyrolysis.<sup>96,97</sup>

One significant challenge with GC is that the pyrolysis process generates a wide range of products, especially when the sample is a polymer, many of which can interfere with the detection of low-concentration additives. This interference makes it difficult to identify and quantify minor additives using FID. More selective detection methods, such as AED or mass-selective detectors, offer better sensitivity for detecting these low-level additives by focusing on specific elements or fragments.<sup>46</sup> For accurate detection, the pyrolysis products must be volatile and have sufficient vapor pressure to travel through the column. High-molecular-weight, polar, or unstable products often cannot be separated or detected through conventional gas chromatography. One approach to mitigate this is online derivatization during pyrolysis, which increases the volatility of certain pyrolysis products and improves their detectability. Additionally, shorter columns, though they sacrifice resolution, have been shown to pass

some polar large molecules that otherwise would not be detected.<sup>98</sup> Another critical requirement in GC is the standardization of experimental conditions. Factors such as pyrolysis temperature, duration, sample size, and carrier gas flow rate must be strictly controlled to ensure reproducibility of results. Small variations in these parameters can lead to inconsistencies in the pyrolysis products formed and detected, affecting both qualitative and quantitative analysis. Lastly, for GC to be effective in quantitative analysis, proper calibration of the detection system is required. Calibration ensures that the detector's response is proportional to analyte concentration, enabling accurate quantification. This process typically involves using internal or external standards, or even polymer-based “pyrolytical standards”, to calibrate the detector. Advanced techniques, such as principal component analysis (PCA), can further enhance the accuracy of quantitative data by considering more complex relationships between the detector response and analyte concentration.<sup>99</sup>

**4.1.2. Recent advances and current trends.** The use of GC-single response detectors for additive analysis is a relatively minor application but has been employed for the quantitative determination of a wide range of additives in polymers. These include UV stabilizers, plasticizers, antioxidants, sulfur-containing compounds, binders in paints, and toners on paper. A variety of detectors, such as FID, NPD, and FPD, have been utilized for these analyses, which have been conducted on both solid samples and extracts. A GC method was developed for the identification of the antioxidant Alurofen in synthetic rubber materials.<sup>100</sup> Sinclair *et al.* used PP extracts in the analysis of DSTDP antioxidant in the concentration range 0.1 to 0.7 wt% DSTDP/polymer.<sup>44</sup> They found that GC, when coupled with pyrolysis and a sulfur-selective detector FPD, enabled precise and reproducible quantification of the additive.<sup>44</sup> This supports the idea that GC, especially when combined with pyrolytic breakdown and selective detection, serves as a powerful tool for identifying and quantifying non-volatile, sulfur-containing additives in polymer matrices, even at low concentrations.

Another method, known as Curie point pyrolysis GC, has been used by Perlstein *et al.* to analyze different low-molecular-weight light stabilizers and HALS extracted from low-density polyethylene (LDPE) and polypropylene (PP) matrices.<sup>45</sup> Curie point pyrolysis is a specialized technique in which a sample is rapidly heated to a specific, constant temperature known as the “Curie point”. By rapidly reaching and maintaining this temperature, the technique ensures highly reproducible thermal degradation of the sample, minimizing thermal gradients and uncontrolled overheating. They found that the pyrolysis products of HALS exhibited distinct and reproducible chromatographic patterns. However, the samples analyzed were formulated with a known amount of additives.<sup>45</sup> This study supports the idea that GC can be used to identify and differentiate HALS based on their thermal degradation profile. While the analysis of high-molecular-weight stabilizers can be challenging due to their thermal instability, in pyrolysis this instability can be utilized to generate distinctive fragments.



GC has been applied to commercial rubbers, allowing simultaneous detection of polymers, heat stabilizers, and plasticizers in a single experiment. For example, step-wise pyrolysis GC-FID has detected and identified butadiene-acrylonitrile rubber, Neozone D stabilizer, and phthalate plasticizers.<sup>43</sup> Step-wise pyrolysis is a thermal degradation approach in which the sample is progressively heated in controlled temperature intervals, releasing volatile components at each stage for GC analysis. This method can also detect differences in the same type of rubber produced by different manufacturers.<sup>101</sup> Moreover, GC is effective in identifying organic binders in paint and detecting various additives like phthalates in automotive and architectural paints, and industrial finishes.<sup>102</sup> These efforts demonstrate the versatility and diagnostic power of GC techniques for comprehensive compositional analysis of complex polymer systems, enabling both qualitative identification and quantitative assessment of additives and polymer types across diverse material sources.

GC paired with single-response detectors, such as FID, NPD, and FPD, remains an effective tool for the analysis of various additive classes, including antioxidants and UV stabilizers. When combined with pyrolysis or selective detection, these setups provide sensitive and reproducible quantification from both solid samples and extracts. While these detectors offer valuable information for monitoring known additives, the literature indicates that their utility is highest when used in conjunction with known reference standards, as they do not provide the structural identification capabilities required for

characterizing unknown additive packages in complex commercial materials.

#### 4.2. Gas chromatography with spectral detectors for polymer additive analysis

**4.2.1. Fundamentals and limitations.** GC combined with detectors such as MS, AED, and FTIR, which provide a spectrum as a response, enables both separation and identification of additives and degradation products, providing retention time, mass fragmentation patterns, elemental, or functional group information. A simplified diagram of the GC technique is shown in Fig. 8. In GC-MS, as the gas compounds enter the mass spectrometer, they are ionized, typically by electron ionization (EI). This ionization process breaks the molecules into charged fragments. Using a mass analyzer, these ionized fragments are then sorted in the magnetic field and detected based on their mass-to-charge ratio ( $m/z$ ).<sup>103</sup> In GC-AED, the separated compounds are introduced into a high-temperature plasma, atomized, and excited; the emitted light at element-specific wavelengths is monitored to determine elemental composition. In GC-FTIR, the separated compounds pass through an IR gas cell, where their absorption spectrum is recorded to provide functional group identification. Pyrolysis GC-MS, GC-AED, and GC-FTIR are widely used for additive analysis because the sharp release of volatiles yields well-resolved chromatograms, and the rapid heating minimizes oxidative side reactions when performed under inert gas. However, the high temperature can still induce secondary reac-



**Fig. 8** (A) A simplified schematic of GC showing the pyrolysis chamber, GC column, and detector. The detector can be single response or spectral. (B) Schematic of the GC-MS system where volatiles get separated in a GC column, ionized on exit, and captured and analyzed via MS.



tions, potentially generating artifacts that complicate identification. In contrast, pyrolysis with mass spectrometry (Py-MS) omits chromatographic separation: the pyrolysis products are transferred directly into the mass spectrometer for rapid analysis. This configuration removes the limitation on maximum detectable molecular mass imposed by GC, enabling the detection of high-molecular-weight species that would otherwise be non-volatile under GC conditions. However, the absence of chromatographic separation means that complex mixtures can produce overlapping mass spectra, reduce specificity, and make deconvolution more challenging.

**4.2.2. Recent advances and current trends.** Characterizing unknown cured epoxy resins requires identifying minor components such as coupling agents and catalysts, which are typically added in small percentages and react with the resin, making them difficult to detect as free compounds. GC, particularly when combined with spectroscopic detectors like MS, FTIR, and AED, helps identify these components by focusing on the distinctive fragments generated during pyrolysis.<sup>104</sup> GC has also been applied to flame retardants in high-temperature engineering thermoplastics, a challenging area due to the difficulty of dissolving these polymers. Wang used GC-AED and GC-MS to analyze various brominated flame retardants in polyesters and polyamides.<sup>46</sup> The key to GC-AED's effectiveness is its ability to detect specific elements, like bromine, by using atomic emission lines, and then match the pyrolysate patterns with known standards. This allows for both identification and quantitative analysis when standards are available. AED is particularly valuable when specific-element detection is required, complementing MS, which excels in fragment analysis. To summarize, research work supports the use of GC for identifying and measuring additives and residual monomers directly within polymer matrices, eliminating the need for prior separation. Pyrolysis GC-MS has become a widely used method for analyzing organic polymer additives (OPA), as it identifies additives through their pyrolytic degradation products.<sup>47</sup> Early applications by Perlstein and Orme (1985) identified and semi-quantified UV stabilizers such as the Tinuvin® and Chimassorb® series and antioxidants such as Irganox® 1010 in polyethylene and polypropylene. However, this method is hindered by overlapping peaks and low recovery rates (72–94%). Moreover, additive identification is often challenged by the abundance of polymer fragments, making direct analysis in complex matrices problematic.<sup>105,106</sup> To address these challenges, multi-step pyrolysis (or multi-shot Py-GC/MS) separates the analysis of additives from polymeric matrices by using sequential temperature stages. The first stage desorbs additives without degrading the polymer, while the second stage analyzes the polymer itself at high temperatures (>500 °C).<sup>107,108</sup> This method simplifies spectra interpretation and facilitates additive identification, as demonstrated in studies by Yanagisawa *et al.* While Py-GC/MS offers rapid analysis without extensive pre-treatment, laboratory contamination from additives such as Irgafos® 168 requires careful material selection to avoid analytical interference.<sup>109</sup>

GC-spectroscopic methods remain central to characterizing additives in polymers because they convert non-volatile or difficult-to-extract compounds, such as catalysts and flame retardants, into identifiable fragment patterns. While element-specific detection with AED and structural elucidation with MS help mitigate the complexity of overlapping signals, interference from abundant polymer fragments continues to limit confident identification in complex materials. Multi-step pyrolysis has significantly improved this analytical bottleneck by temporally separating additive desorption from bulk polymer degradation. This separation produces cleaner chromatograms and more interpretable data, which facilitates both qualitative identification and quantitative accuracy in the analysis of real-world polymer formulations.

### 4.3. HPLC for polymer additive analysis

**4.3.1. Fundamentals and limitations.** HPLC is a powerful technique for quantitatively analyzing and separating mixtures in solution.<sup>110</sup> In this method, the sample is injected into the mobile phase, which then interacts with the stationary phase, which can vary in type. The stationary phase may be polar, such as silica gel, or non-polar, such as silica coated with hydrophobic groups. Ion-exchange columns and size-exclusion columns can also be utilized. As the liquid mobile phase is mixed with the sample solution and pumped through the stationary column, the components of the mixture are separated based on their relative affinities for the stationary phase. This separation results in each component being eluted at different times, known as retention times.<sup>111</sup> A detector is placed at the end of the system to analyze the solution as it elutes from the column. The concentration of the individual component is proportional to the area under the signal-intensity curve.<sup>112</sup> A schematic of an HPLC system is shown in Fig. 9.

**4.3.2. Recent advances and current trends.** HPLC is more suitable than GC for non-volatile additives. While gas chromatography employs both sensitive and universal detectors, the technique faces limitations due to the high molecular weight and polar nature of many antioxidants and light stabilizers, which tend to decompose at elevated temperatures needed to produce the vaporized samples for GC.<sup>113</sup> However, most antioxidants have chromophores that allow detection by UV, making HPLC-UV a facile route for their analysis. Thilén *et al.* demonstrated that HPLC UV could be used to quantify known additives in a known polymeric system.<sup>51</sup> They mixed a non-stabilized polypropylene with Irganox 1010 and Irgafos 168 and later supercritically extracted them to analyze by HPLC UV using a methanol/water system as the mobile phase. They compared peak intensities with the standards to determine that the concentration was between 1450 to 1850 ppm.<sup>51</sup> In contrast, Demertzis *et al.* used an acetonitrile/THF system as the mobile phase to quantify known additives such as Irganox 245, Irganox 1035, Irganox 1098, and Irganox 3114 by HPLC UV during stability testing of these antioxidants in food simulants.<sup>48</sup> They were able to measure concentrations of these additives between 3 and 45 ppm.<sup>48</sup>





**Fig. 9** Simplified schematic of an HPLC system showing the mobile phase that carries the injected sample through the stationary column, where analytes are separated before detection and recording of retention times.

HPLC-UV has also been used to analyze polymers with unknown additives. For example, El Mansouri *et al.* successfully extracted and detected di-*tert*-butyl phenol (DTBP), hindered amine light stabilizers (Tinuvin 326), hindered phenolic antioxidants (Irganox 1010), and phosphorous antioxidants (Irgafos 168 and Ultrinox 626), along with their degradation products from commercial polypropylene. They were able to quantify the additives by comparing signal intensities with those of standards.<sup>49</sup> In contrast to detectors that monitor only one UV wavelength, a photodiode array (PDA) detector can scan a range of wavelengths. Li *et al.* used UV PDA detectors to detect and quantify unknown additives in commercial food packaging films of different polymer types, including PE, PP, and multilayer composites. A wide range of standards representing antioxidants, UV stabilizers, and phthalate plasticizers were prepared in methanol or toluene/methanol to generate calibration curves and establish retention times and UV spectra. Detection was carried out at 276 nm, and additives in the film extracts were identified and quantified by matching retention times and spectra with standards. This workflow enabled the accurate determination of multiple additives in real-world packaging matrices.<sup>50</sup>

HPLC serves as a critical alternative for the analysis of non-volatile, thermally unstable, or polar additives where GC-based techniques are fundamentally limited. The literature demonstrates that by pairing selective extraction with UV or PDA detection, researchers can achieve reliable quantification and identification of unknown additives and their degradation products within complex matrices. However, a comparative look at the literature reveals a significant adoption gap. While hyphe-

nated techniques such as HPLC-MS provide superior structural detail and shorter analysis times, their higher operational costs and lower accessibility compared to standard HPLC configurations remain a primary constraint. Consequently, standard HPLC remains the most widely implemented tool for routine quantification, while HPLC-MS is reserved for scenarios requiring high-resolution structural elucidation.

Chromatographic methods represent the most robust approach for the separation and quantification of complex additive packages. Because these techniques resolve the molecular-level overlaps that frequently hinder spectroscopic analysis, they serve as the definitive characterization stage within the proposed roadmap (section 8). In this framework, the strategic selection between GC and HPLC is based on additive volatility and thermal stability; consequently, these methods are best employed after the specific additive, or its chemical family, has been tentatively identified. Ultimately, coupling chromatography with spectroscopic detectors allows for confident molecular identification even in complex, unknown systems.

## 5. Elemental analysis

Elemental analysis, such as carbon/hydrogen/nitrogen/sulfur (CHNS) analysis, inductively coupled plasma (ICP) analysis, and energy dispersive X-ray spectroscopy (EDS) is widely employed to quantify the loading and distribution of elements in polymeric materials. These techniques can reveal information about polymer additives that contain the specific



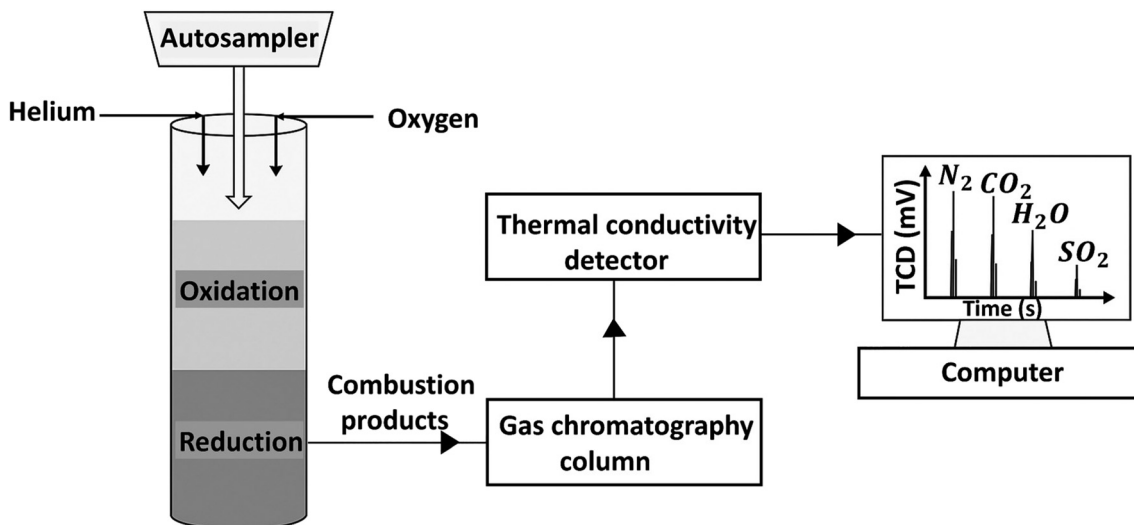


**Fig. 10** Simplified diagram of CHNS elemental analyzer, where the sample is combusted, the resulting gases are separated by a gas chromatography column eluting to a thermal conductivity detector.

element or elements detected. CHNS analysis relies on combustion-based techniques to determine the relative amounts of carbon, hydrogen, nitrogen, and sulfur in a sample, making it useful for verifying the presence of stabilizers, plasticizers, or flame retardants containing these elements. ICP techniques, including ICP-OES (Optical Emission Spectroscopy) and ICP-MS (Mass Spectrometry), involve the ionization of elements in a high-temperature plasma, allowing for highly sensitive and precise detection of additives containing trace amounts of metals. EDS, often integrated with scanning electron microscopy (SEM-EDS), provides spatially resolved elemental composition by detecting characteristic X-rays emitted from a sample upon electron beam excitation, making it particularly effective for mapping inorganic additives and fillers in a polymer matrix.

### 5.1. CHNS for polymer additive analysis

**5.1.1. Fundamentals and limitations.** CHNS elemental analysis is a well-established method for quantifying the content of carbon (C), hydrogen (H), nitrogen (N), and sulfur (S) in organic compounds. A simplified diagram of CHNS elemental analyzer is illustrated in Fig. 10. The technique begins with the oxidation of the polymer sample in a high-temperature furnace under an oxygen-rich atmosphere, ensuring complete combustion. This oxidation process breaks down the sample into its elemental components, producing combustion gases such as  $\text{CO}_2$ ,  $\text{H}_2\text{O}$ ,  $\text{N}_2$ , and  $\text{SO}_2$ . The presence of oxygen ensures that carbon and hydrogen are oxidized to  $\text{CO}_2$  and  $\text{H}_2\text{O}$ , while nitrogen and sulfur are converted to  $\text{N}_2$  and  $\text{SO}_2$ , respectively.<sup>114</sup> After combustion, the resulting gases are carried by an inert carrier gas, typically helium, through a gas chromatographic system for separation. Helium is chosen as a carrier gas due to its inert nature, low molecular weight, and high thermal conductivity, which make it ideal for transporting analytes without interference. During the separation

process, each gas species is isolated based on its interaction with the gas chromatography (GC) column material and its volatility. Once separated, the gases are detected and quantified using a thermal conductivity detector (TCD). The TCD measures changes in thermal conductivity between the carrier gas (helium) and the combustion products. As each gas exits the column and passes over the TCD's heated filament, its thermal conductivity affects the filament's temperature and electrical resistance. These changes generate a signal that corresponds to the concentration of the specific gas. The signals from  $\text{CO}_2$ ,  $\text{H}_2\text{O}$ ,  $\text{N}_2$ , and  $\text{SO}_2$  are used to calculate the amounts of carbon, hydrogen, nitrogen, and sulfur in the original sample, providing precise quantitative data.<sup>115</sup> In this process, oxidation plays a critical role in breaking down the sample, while reduction may occur in secondary reactions or specific analytical setups (e.g., reducing  $\text{NO}_x$  to  $\text{N}_2$  for nitrogen detection).<sup>116</sup> A primary advantage of CHNS analysis is its high level of precision in quantifying organic additives. For polymers containing heat stabilizers, plasticizers, or flame retardants that include these elements, CHNS analysis provides accurate and reproducible data. The method is particularly effective for analyzing additives based on nitrogen and sulfur, such as nitrogen-based antioxidants or sulfur-containing flame retardants. However, CHNS analysis has several limitations. As a bulk technique, it provides only the overall elemental composition of the polymer, without offering spatial information about additive distribution. This lack of spatial resolution is a significant drawback when additives are non-uniformly distributed or localized in specific regions, particularly in applications where such localization critically affects the polymer's performance. Additionally, CHNS analysis is destructive: the polymer sample is completely consumed during combustion. This makes it impossible to perform further analyses on the same sample. Another limitation is the narrow range of elements that CHNS can detect. While the



technique is excellent for analyzing C, H, N, and S, it is not applicable for elements such as phosphorus (P) or chlorine (Cl), which are common in certain types of polymer additives such as antioxidants.<sup>117</sup> Moreover, due to the high carbon and hydrogen content in most polymers, the CHNS technique is generally not effective for identifying or quantifying additives based on C and H, and is typically only sensitive to additives containing nitrogen or sulfur. As a result, CHNS analysis often needs to be complemented by other techniques, such as ICP-OES or gas chromatography-mass spectrometry (GC-MS), to obtain a complete picture of the additive composition. Despite these challenges, CHNS remains a viable technique for quantifying organic additives in polymers. When combined with non-destructive methods such as FTIR spectroscopy, it offers a more comprehensive understanding of both the composition and spatial distribution of additives within the polymer matrix.

**5.1.2. Recent advances and current trends.** Cuthbertson *et al.* characterized 59 polymers from common commercial vendors across 20 polymer classes using a series of techniques, including CHNS for elemental analysis, despite the composition of the additives being unknown.<sup>52</sup> The authors reported elements measured at >0.005 wt% and noted elements present in trace amounts (<0.004 wt%). They also attributed elements observed at trace levels ( $\ll 0.004$  wt%) to contaminants introduced during plastic processing or trace amounts of excess catalyst. However, without targeted analysis of specific inorganic additives, they could only make inferences about the possible additives present, given the specific elements present. For example, while CHNS quantified sulfur content in polymers (*e.g.*, 0.1–0.8 wt% in some samples), it could not distinguish between different sulfur-containing additives or identify their specific chemical forms. For instance, sulfur may originate from various additives such as mercaptans, thiols, or sulfonamides. Without complementary techniques like GC-MS, CHNS alone could not confirm the presence of specific compounds.<sup>52</sup> This study demonstrates that while CHNS could be used to make inferences about possible additives in polymeric system, it could not specify exact additives present without the help of complementary techniques. Habib *et al.* applied the CHNS technique to investigate the chemical changes in bitumen before and after melt-blending with polypropylene (PP) at varying concentrations.<sup>118</sup> A significant increase in oxygen content was observed in all PP-modified bitumen samples, suggesting the formation of ketones, phenols, or carboxylic acids. The presence of these compounds may contribute to pavement deterioration through aging.<sup>118</sup>

Liang *et al.* measured the sulfur content in recycled styrene-butadiene rubber ground tire rubber using a CHNS analyzer.<sup>53</sup> Sulfur content serves as a reliable indicator correlated with cross-link density, providing valuable insight into the quality and performance of recycled tire rubber.<sup>53</sup> Similarly, CHNS analysis has been employed to quantify sulfur-containing flame retardants in polymeric materials. Jia *et al.* conducted elemental analysis on a synthesized sulfur-containing cyclophosphazene and correlated the effects of phosphazene deriva-

tives on the polymer's refractive index and flame retardancy by determining the elemental content.<sup>119</sup> This study demonstrates that the CHNS technique is a valuable tool for guiding the synthesis of sulfur-containing flame retardants. Moreover, Hu *et al.* also utilized CHNS analysis to determine drug loading in polymeric prodrugs.<sup>54</sup>

Elemental analysis (CHNS) provides a reliable means for the quantitative monitoring of additive loading and the tracking of chemical transformations within polymer systems. While these techniques provide precise measurements of total elemental content, such as sulfur or oxygen levels, they remain fundamentally inferential regarding specific chemical identities. For example, elemental data can indicate changes in cross-link density, guide the synthesis of flame retardants, or monitor the formation of degradation products, but it cannot distinguish between different molecular species without the support of complementary structural elucidation tools. Consequently, elemental analysis is best utilized as a foundational quantitative method to establish an elemental fingerprint, which must then be integrated with qualitative techniques to achieve definitive additive identification in complex formulations.

## 5.2. ICP for polymer additive analysis

**5.2.1. Fundamentals and limitations.** ICP techniques are powerful analytical methods for detecting and quantifying trace elements in a sample. In all cases, the sample is first ionized using an inductively coupled plasma. The detection step then determines the specific type of ICP technique being used: if a mass spectrometer analyzes the resulting ions, the method is called ICP-MS; if the light emitted by the excited ions is analyzed instead, the method is known as ICP-OES. Fig. 11(A) depicts a simplified ICP-MS/OES setup, and Fig. 11 (B) shows the formation of ions and radiation in the plasma that are directed to MS or OES for analysis. In both methods, the first critical step when analyzing solid polymer samples is sample preparation, which involves breaking down the polymer matrix into low-molecular-weight, soluble fractions. This is typically achieved by dissolving or digesting the polymer in a closed microwave digestion system using a mixture of strong acids. This process not only ensures that the sample can pass through the spray chamber but also helps retain volatile analyte species that might otherwise be lost. Once properly digested, the resulting solution is introduced into a nebulizer, where it forms a fine aerosol with argon gas. The aerosol then enters the spray chamber, which filters out larger droplets and allows only fine particles to proceed into the core of an inductively coupled argon plasma, where temperatures reach approximately 9000 K. At these high temperatures, the sample is vaporized, and the analyte species are atomized, ionized, and thermally excited, making them suitable for subsequent detection and quantification. At this point, the two techniques diverge in their detection systems. In ICP-MS, the ions are directed into a mass spectrometer, where they are separated based on their mass-to-charge ratios, allowing for ultra-trace detection down to 1–10 ppt.<sup>120,121</sup> In contrast,



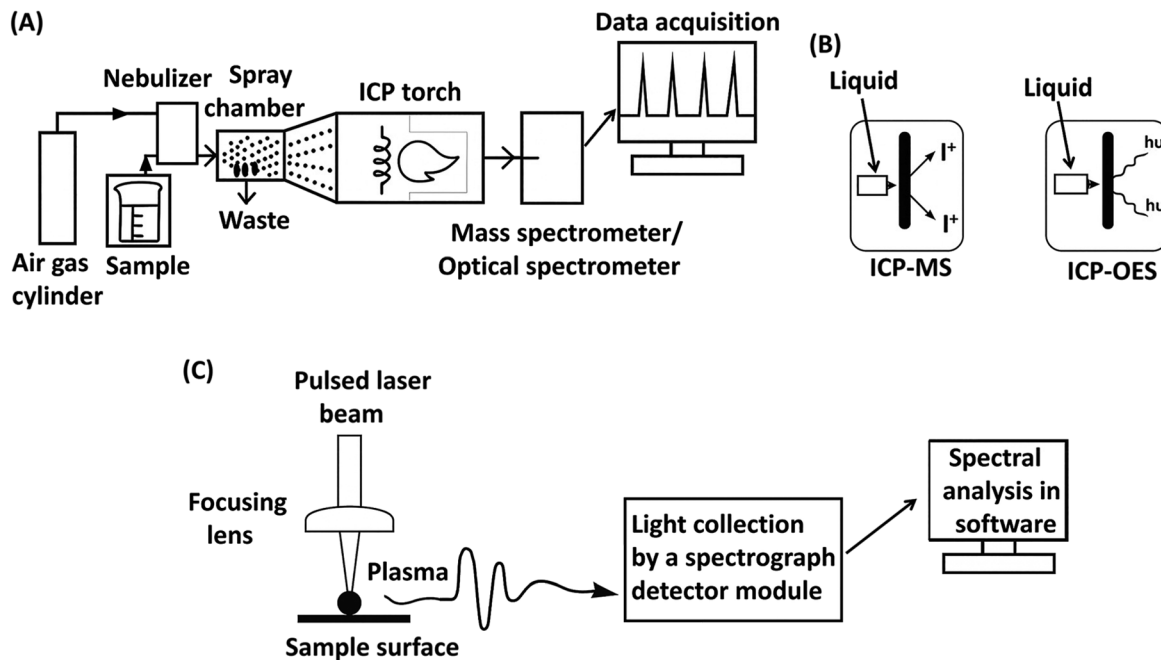


**Fig. 11** (A) A simplified schematic of ICP-MS/OES, where the sprayed sample is introduced into an ICP torch and analyzed by a mass or optical spectrometer, (B) processes occurring after the torch, with ion formation leading to mass spectrometry (MS) or photon emission leading to optical emission spectrometry (OES), (C) a simplified diagram of LIBS, where plasma emission is collected and analyzed spectroscopically.

ICP-OES relies on the optical emission of light from excited atoms returning to lower energy states. The emitted light is measured using optical emission spectrometer at characteristic wavelengths, with detection limits typically in the 1–10 ppb range.<sup>122,123</sup> The measurements using this spectrometer are converted to elemental concentration by comparison with calibration standards.

However, most polymers are highly resistant to chemical breakdown, resulting in incomplete digestion and reduced nebulization efficiency. To analyze these materials, solid-sampling techniques like Laser Ablation Inductively Coupled Plasma Spectrometry (LA-ICP-MS/OES) and Laser-Induced Breakdown Spectroscopy (LIBS) are typically used. This technique eliminates the need for sample preparation, offering rapid and spatially resolved analyses. However, in these techniques, the absence of certified reference materials for polymers poses challenges for calibration, leading to the common practice of using polymer samples characterized by alternative methods.<sup>124–127</sup> LA-ICP-MS/OES begins by directing a focused laser beam onto the surface of the solid sample, where it ablates material to form fine particles. An inert gas then carries these particles into the inductively coupled plasma, where they are vaporized, atomized, and ionized before being analyzed by a mass spectrometer or an optical spectrometer for elemental analysis.

In LIBS, a short laser pulse is focused onto the sample surface, ablating a small amount of material and forming a high-temperature plasma that can exceed 30,000 K. This plasma contains free electrons, excited atoms, and ions. Once the laser pulse ends, the plasma begins to cool rapidly. As it

cools, the excited atoms and ions return to their ground states, emitting light at element-specific wavelengths. This emitted light is then collected and analyzed by a spectrograph and detector to determine the sample's elemental composition. A simplified diagram of LIBS is shown in Fig. 11(C).

Although ICP can be used to infer the presence of additives at very low concentrations in polymers, it is an elemental analysis technique. It thus provides no information about the molecular structure. In ICP-MS, mass spectral interferences from matrix elements, polyatomic species, isobaric overlaps, and multiply charged ions can complicate the accurate quantification of some analytes. ICP-OES, on the other hand, may suffer from spectral interferences if emission lines of different elements are too close or overlap. Halogen determination by ICP-MS is analytically challenging due to their high ionization energies, low ionization efficiencies in argon plasma (particularly for fluorine), and numerous spectral interferences formed in the Ar plasma.<sup>128</sup> In particular, Ar-based polyatomic ions such as  $^{36}\text{Ar}^1\text{H}^+$  (mass 37) and  $^{40}\text{Ar}^{40}\text{Ar}^1\text{H}^+$  (mass 81) directly overlap with and interfere with the detection of  $^{37}\text{Cl}^+$  and  $^{81}\text{Br}^+$ , respectively. These interferences can compromise accuracy when using conventional ICP-MS. However, many of these limitations can be addressed with modern instrumentation. High-resolution ICP-MS and sector-field (HR-ICP-SF-MS) instruments can resolve key overlaps by operating at medium or high mass resolution ( $m/\Delta m \approx 4000\text{--}10\,000$ ), allowing interference-free measurement of halogen isotopes such as  $^{35}\text{Cl}^+$ ,  $^{37}\text{Cl}^+$ ,  $^{81}\text{Br}^+$ , and even  $^{19}\text{F}^+$ .<sup>129</sup> Collision/reaction cell systems, alternative plasma gases (e.g., He plasma for fluorine), and improved ion optics further enhance sensitivity and reduce



background signal.<sup>130</sup> Contrary to ICP-MS/OES, ICP-LIBS primarily analyzes the surface or near-surface region of the sample. While it can perform depth profiling, this requires multiple pulses and careful control and may not accurately represent the bulk composition. However, these techniques are useful for detecting metals and other elements associated with the additives that could not be extracted from the polymer matrix for HPLC analysis or vaporized for GC-MS detection.

**5.2.2. Recent advances and current trends.** Pereira *et al.* determined concentrations of elements such as As, Bi, Cd, Co, Cu, Hg, Mn, Mo, Ni, Pb, Sb, Sr, Ti, V, and Zn using ICP-MS and ICP-OES.<sup>55</sup> In this study, they compared two sample preparation methods, namely microwave-induced combustion (MIC) and microwave-assisted acid digestion (MW-AD), for digesting various polymers to measure trace elements (*e.g.*, As, Cd, Pb, Zn) using ICP-MS and ICP-OES. They tested six commercial polymers: LDPE, HDPE, PP, PS, PET, PEEK, and nylon 6,6. MIC was found to be superior due to its ability to use diluted acids, digest larger sample masses, and produce lower residual carbon, leading to better detection limits. MIC also offered faster processing time (25 min) compared to MW-AD (>50 min).<sup>55</sup> This study demonstrates how ICMS/OES methods combined with robust sample preparation, particularly microwave-induced combustion (MIC), can effectively detect and quantify elemental additives or contaminants in real-world, compositionally unknown polymer samples. Notably, the study highlights that sample preparation is a critical step in trace elemental analysis of polymers, directly impacting detection limits, accuracy, and overall data reliability.

On the other hand, Hemmerlin *et al.* prepared a series of six in-house PVC reference materials by incorporating various additives at increasing concentrations and utilized LA-ICP-OES to obtain satisfactory results and good agreement for seven of the ten incorporated elements (Al, Ca, Cd, Mg, Sb, Sn, and Ti).<sup>56</sup> They also confirmed sample homogeneity and presented calibration graphs for several elements using LA-ICP-OES.<sup>56</sup> However, techniques such as LA-ICP-MS/OES and LIBS are highly sensitive to matrix effects, where differences in the chemical and physical properties of different polymers can significantly affect the accuracy of analyte determination within the polymer. As a result, accurate quantification with these methods typically requires matrix-matched reference materials. This becomes a major limitation when analyzing unknown polymers, as it is often impractical to prepare or obtain reference standards tailored to each possible polymer. Bonta *et al.* studied a tandem LA-ICP-MS/LIBS procedure enhanced with statistical analysis.<sup>131</sup> While LIBS is particularly prone to matrix effects, they leveraged its complete broadband spectra as signatures for the analyzed polymer types, including polyimide, polymethylmethacrylate, and polyvinylpyrrolidone, to mitigate these effects. This approach enabled the detection of alkali metals and other trace metals, resulting in multivariate calibration models with reasonable accuracy, with validation showing relative average deviations from the actual elemental content of just 4.4% and no more than 9.6%.<sup>131</sup>

The literature indicates that while ICP-MS and ICP-OES can reliably quantify trace elemental additives across diverse polymers, their success depends heavily on rigorous sample preparation, particularly microwave-induced combustion. In contrast, laser-based methods such as LA-ICP-OES and LA-ICP-MS offer the advantage of direct elemental profiling but are constrained by significant matrix effects. Consequently, meaningful quantification with laser-based techniques generally requires polymer-specific reference materials. While emerging multivariate strategies that combine LA-ICP-MS and LIBS can mitigate these matrix dependencies and improve predictive accuracy, such approaches remain contingent upon the availability of well-characterized calibration sets. Collectively, these findings suggest that the choice between solution-based and laser-based elemental analysis involves a direct trade-off between processing speed and the necessity for matrix-matched standards.

### 5.3. SEM-EDS for polymer additive analysis

**5.3.1. Fundamentals and limitations.** EDS is a technique based on the interaction of high-energy electrons with atoms, which leads to the emission of characteristic X-rays that are detected and analyzed.<sup>132</sup> A simplified diagram of EDS detector is illustrated in Fig. 12. When a high-energy electron beam is directed at the sample, it excites the atoms, causing them to emit X-rays at specific energies corresponding to their atomic number. These emitted X-rays are then detected and analyzed to identify the elements present within the sample. EDS is frequently used in combination with scanning electron microscopy (SEM) to provide both morphological and elemental data.<sup>133</sup> One of the main advantages of EDS is its non-destructive nature, meaning the polymer sample remains intact after analysis. This is especially beneficial when further testing or analysis is required on the same sample. Additionally, EDS provides spatially resolved elemental mapping, allowing researchers to visualize the distribution of additives within the polymer matrix. EDS, equipped with modern silicon drift detectors (SDDs), can detect a wide range

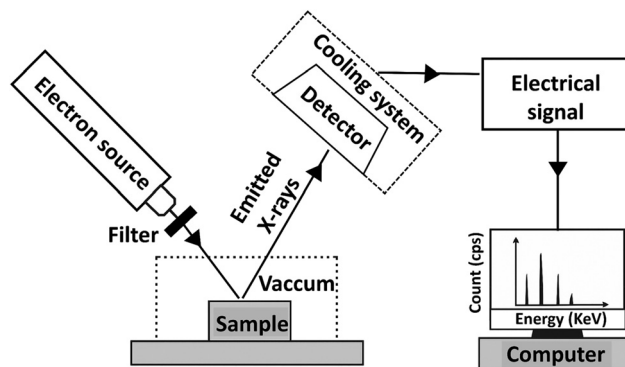


**Fig. 12** Simplified schematic of an energy-dispersive X-ray spectroscopy (EDS), showing the generation of X-rays from an electron beam-sample interaction, detection of the emitted X-rays, and conversion into an electrical signal for spectral analysis.



of elements, both qualitatively and quantitatively, covering atomic numbers from 5 (boron) to 92 (uranium), making it highly versatile for analyzing additives such as flame retardants, fillers, and stabilizers.<sup>134</sup> The application of EDS in detecting polymer additives is particularly useful for detecting inorganic additives, including metal-based stabilizers, flame retardants, catalysts, and residues from processing aids. For instance, bromine (Br) and chlorine (Cl), which are commonly used in halogenated flame retardants,<sup>135</sup> can be effectively detected using EDS. Nickel chelates, commonly used for their UV absorption and radical scavenging properties,<sup>136</sup> can be identified by the distinct nickel signal in the EDS spectrum. While EDS provides elemental data, it is often used alongside complementary techniques, such as FTIR spectroscopy and NMR spectroscopy, to confirm the presence and chemical structure of these stabilizers within polymer matrices. EDS faces several challenges in the context of polymer additive identification and quantification. The technique's sensitivity is often insufficient for detecting low concentrations of additives/elements, which is a limitation when analyzing trace-level components.<sup>137</sup> Older non-SDDS-based systems fail to detect carbon (C) and nitrogen (N), common elements in many polymer additives, and even modern EDS equipped with SDDS struggle to detect hydrogen (H). This limitation is due to the lower energy of X-rays emitted by these elements, which is often not detected efficiently.<sup>138</sup> Thus, the applicability of EDS to polymer additives was enhanced by the introduction of SDDS in the early 2000s. EDS is also a surface-sensitive technique, providing information primarily about the surface composition of the polymer.<sup>139</sup> For polymer systems where the bulk composition differs significantly from the surface, this can lead to inaccurate conclusions about additive distribution. To obtain information about the bulk composition, sample cross-sectioning or additional techniques are required. Combining EDS with other techniques, such as transmission electron microscopy (TEM) or CHNS analysis, can provide a more comprehensive view of polymer composition, particularly when dealing with both organic and inorganic additives. As the field of polymer science continues to evolve, the role of EDS in additive quantification will likely expand, particularly in the development of advanced composites and sustainable polymers.

**5.3.2. Recent advances and current trends.** Holbrook *et al.* investigated the detection of a commonly used flame retardant, the deca-congener of polybrominated diphenyl ether (BDE 209), in high impact polystyrene (HIPS) using EDS.<sup>58</sup> They detected the presence of bromine in a television casing sample, consistent with HIPS formulations that typically contain BDE 209 powder. However, definitive identification and quantification of the additive required complementary techniques such as GC-MS. The results demonstrated that EDS is a promising technique for the elemental and chemical detection of brominated flame-retardant compounds in polymeric materials, which is important for determining routes for the removal of organic pollutants from the environment.<sup>58</sup> Fries *et al.* conducted a study to detect and identify unknown

inorganic additives in unknown marine microplastic particles using an EDS detector coupled with SEM.<sup>59</sup> Titanium was detected on the surface of the microplastic and attributed to titanium dioxide nanoparticles originating from white pigments or UV blockers added during polymer manufacture.<sup>59</sup> Dvir *et al.* determined the spatial distribution and the extent of polymerization of the pentabromobenzylacrylate (PBBMA) flame retardant in PP using EDS. This research highlights EDS as a powerful tool to evaluate not only the distribution of the flame retardant but also the compatibility between the PP matrix and polar fillers, achieved by detecting and analyzing the extent of PBBMA polymerization.<sup>57</sup>

Again, EDS is also frequently used to quantify mineral fillers, such as calcium carbonate (CaCO<sub>3</sub>), zinc oxide (ZnO), and silica (SiO<sub>2</sub>), in polymers. These fillers are often added to improve mechanical properties and reduce costs. Won *et al.* prepared additively manufactured resin nanoceramics (RNCs) with varying proportions of barium silicate filler: 0 wt% barium silicate and 100 wt% polymer (B0/P10, control group), 50 wt% barium silicate and 50 wt% polymer (B5/P5), 60 wt% barium silicate and 40 wt% polymer (B6/P4), and 67 wt% barium silicate and 33 wt% polymer (B6.7/P3.3).<sup>60</sup> These specimens were then examined using scanning electron microscopy (SEM) and energy-dispersive X-ray spectroscopy (EDS) to investigate filler distribution within the polymer matrix. The B6/P4 group showed elliptical ceramic crystal aggregates with higher Si and O concentrations and lower C compared to the surrounding matrix, indicating localized enrichment of silicate phases. By contrast, the B6.7/P3.3 group exhibited a more uniform mixing pattern, with EDS confirming higher overall Si and O contents and lower C content than the B6/P4 group. Although the authors did not provide absolute quantification of elemental content, they conducted a comparative assessment across groups, allowing them to distinguish between localized enrichment and more uniform filler distribution.<sup>60</sup> These findings highlight the utility of SEM-EDS for comparative quantification of additive dispersion in polymer composites.

These findings indicate that SEM-EDS is most effectively used for elemental screening and mapping additive dispersion, rather than as a primary tool for definitive additive identification. While the technique can confirm the presence of diagnostic elements such as bromine or titanium and evaluate the spatial distribution of mineral fillers, it cannot distinguish among different chemical compounds that contain the same elemental markers. Consequently, SEM-EDS serves a specialized role in evaluating phase compatibility and filler uniformity, but it remains a non-definitive method for structural characterization. This limitation necessitates integrating molecular techniques, such as GC-MS or vibrational spectroscopy, to move from localized elemental detection to precise chemical identification in complex polymer formulations.

Elemental techniques provide a necessary quantitative foundation by establishing an 'elemental fingerprint' of the polymer system. While they lack molecular specificity, they significantly narrow the search space for unknown additives. In the systematic framework in Section 8, these methods serve as



a vital bridge between initial physical screening and final molecular identification, particularly when the additive is unknown prior to analysis.

## 6. Polymer property methods

While spectroscopic, elemental, and chromatographic methods provide direct identification of polymer additives, property-based methods offer a distinct category of analytical insight. Rather than determining specific chemical structures or elemental compositions, these techniques infer the presence of additives by measuring their influence on the polymer's thermal, mechanical, or structural properties. This category encompasses methods such as thermogravimetric analysis (TGA), differential scanning calorimetry (DSC), and X-ray diffraction (XRD). For instance, TGA monitors mass loss as a function of temperature to infer the presence of thermal stabilizers or flame retardants, while DSC detects shifts in glass transition ( $T_g$ ) or melting ( $T_m$ ) temperatures that suggest plasticization or nucleation. However, these techniques provide indirect evidence and cannot definitively identify a specific chemical entity without complementary analytical data. Similarly, XRD reveals modifications in crystalline structure or the formation of new phases, reflecting additive-induced effects rather than direct chemical identity. Collectively, these property-based techniques provide an inferential framework for additive analysis by characterizing the resulting modifications to the polymer matrix.

### 6.1. TGA for polymer additive analysis

**6.1.1. Fundamentals and limitations.** TGA measures the mass loss of a given sample as a function of temperature. The equipment uses a high-precision microbalance in a temperature and atmosphere-controlled oven. The furnace, and thus the sample, is heated at a controlled rate. As the sample degrades and degradation products volatilize, the weight changes are recorded. The atmosphere can be oxygen-depleted (e.g., pure  $N_2$  or Ar) or standard air. Thus, purely thermal and thermo-oxidative degradation behavior can be determined. A simplified diagram of TGA is shown in Fig. 13(A).<sup>140</sup> Several processes can occur as the furnace temperature is raised during the analysis. Low-molecular-weight species, such as residual solvents or additives, may volatilize. Adsorbed species desorb from the polymer surface and then volatilize. Finally, the polymer itself undergoes thermal or thermo-oxidative degradation depending on the atmosphere. The resulting degraded products can then volatilize, leading to a continuous reduction in mass that is recorded as a TGA curve. Additionally, the first derivative of the TGA curve (DTG) provides insight into decomposition kinetics. Representative TGA and DTG curves are shown in Fig. 13(B). The thermal decomposition of polymers can be affected by the presence of some additives.<sup>62</sup> The shifts in degradation temperature, additional mass loss events, and increases in residual masses can all indicate the presence of additives. With the development of libraries for known polymers and additives, it is possible to detect and quantify many additives in polymers using TGA. However, identifying the presence of specific additives in a sample of unknown origin is difficult as there are a plethora



**Fig. 13** (A) Basic schematic of TGA where the sample is heated under controlled conditions and weight changes are recorded by a balance. (B) The resulting data is displayed as a TGA curve (weight loss vs. temperature) and its derivative (DTG curve).



of polymers and additives with overlapping volatilization and degradation behaviors. Thus, TGA is limited to the case where the components of the blend are known, while the exact composition may not be. Coupling TGA with other spectrographic and chromatographic techniques can overcome this limitation by providing information on the evolved gas chemical composition, as discussed in Section 7.

**6.1.2. Recent advances and current trends.** One class of additives that is particularly suited for detection *via* TGA is flame retardants, as they directly impact the oxidative degradation behavior of the matrix polymer. An example of this is found in the work of Sałasińska *et al.*<sup>61</sup> Known flame retardants, fillers, and polymer were mixed to determine the impact on the thermal stability of the compound. High-density polyethylene was used as the matrix. Nanoclay and multiwalled carbon nanotubes were used as fillers. The halogen-free flame retardants examined included zinc borate (FIREBRAKE® ZB), aluminum hydroxide (Reflamal S30), dizinc pyrophosphate (Z 34-80), melamine orthophosphate (MO), and sodium bicarbonate (SB), obtained from various suppliers. Additionally, the halogenated flame retardant decabromodiphenyl oxide (Saytex 102E) was tested. The total additive loading to the polymer was 30 wt%. TGA curves revealed significantly altered degradation patterns compared to the neat polymers. These changes included shifts in onset degradation temperature, residue content, and multi-step degradation behavior indicative of additive influence. However, these studies were largely qualitative. While they demonstrated the potential for correlating degradation temperature or residue content with additive content, they did not develop detailed calibration curves to quantitatively link additive loading to thermal behavior.<sup>61</sup> This suggests that TGA can provide useful insights for qualitative measurements when the additive is known and the loading is high. Losic *et al.* developed a TGA-based method to detect additives in polymers containing graphene counterfeits.<sup>62</sup> They demonstrated that TGA can be used for both qualitative and quantitative detection of carbonaceous counterfeits in graphene materials. They first established baseline TGA/DTG profiles for pure carbon materials like few-layer graphene (FLG), graphene oxide (GO), reduced graphene oxide (rGO), and potential counterfeit additives (*e.g.*, graphite, carbon black, biochar, activated carbon) which were included because these low-cost carbonaceous fillers are sometimes fraudulently blended into graphene products to artificially increase weight and apparent yield, thereby inflating their market value. These materials showed distinct DTG peak shapes,  $T_{\max}$  values, and decomposition ranges, which served as unique thermal “fingerprints”. Here,  $T_{\max}$  refers to the temperature at which the maximum rate of weight loss occurs during decomposition, corresponding to the peak of the DTG curve. When counterfeit carbon materials were mixed with graphene (at 10% concentration), changes in the DTG curves could still be detected and differentiated from pure graphene materials. This enabled qualitative identification of additive presence based on peak position and shape. For quantitative analysis, they used the relative DTG peak intensities to estimate the number of addi-

tives, though results varied slightly due to other impurities. The authors further enhanced the resolution of overlapping peaks by using second-derivative DTG (D2TG) curves and reducing the heating rate from 10 to 2.5 °C min<sup>-1</sup>, thereby helping distinguish materials such as carbon black from graphene. The detection limit was confirmed to be as low as 1% for graphite in graphene, and double-blind testing across instruments and operators confirmed method reproducibility. They also compared the TGA method with XRD and Raman spectroscopy. XRD showed limited capability to detect carbon counterfeits, as most carbon additives exhibited significant peak overlap with graphene, making them indistinguishable at 10% concentration. Similarly, Raman spectroscopy failed to differentiate the additives because common D and G bands were present across graphene, graphite, and other carbon materials.<sup>62</sup> This is an example of how TGA provides a clear advantage in detecting carbon counterfeits, even at low concentrations.

In contrast to these studies where the additive was known, Cuthbertson *et al.* utilized TGA to detect if any additives were present in the commercial polymers polyethylene, polyethylene terephthalate, polypropylene, polyvinyl chloride, polystyrene, polyurethane, acrylonitrile butadiene styrene, nylon, polymethyl methacrylate, polycarbonate, polyvinyl acetate, ethylene vinyl acetate, polyvinyl alcohol, ethylene vinyl alcohol, polycarbonate, polylactic acid, polyacrylonitrile, polybutylene terephthalate, polyketone, polyhydroxybutyrate, and styrene acrylonitrile.<sup>52</sup> They compared the mass loss in air and nitrogen environments as an indication of the presence of additives. Residual mass after thermal degradation suggested the presence of inorganic or thermally stable components such as flame retardants or metal-based additives. By comparing weight loss under nitrogen and air environments, the study distinguished between carbonaceous residues and inorganic materials. Most polymers showed high residue under nitrogen but dropped to <0.3 wt% under air, indicating that the residues were mainly combustible carbon-based materials. However, one of the EVA samples and one of the PVC samples retained significant residue even under air (11% and 8%, respectively), suggesting the presence of oxidatively stable flame retardants or inorganic additives. This was supported by ICP-MS analysis, which confirmed high concentrations of titanium in these samples, indicating the presence of Ti-based flame-retardant additives.<sup>52</sup>

These studies suggest that TGA can be effectively used to screen polymer samples for the presence of additives based on thermal stability and residual mass. However, the technique remains fundamentally inferential; it does not explicitly identify the chemical structure of an additive but instead indicates the presence of thermally stable or inorganic components through observed thermal anomalies. While advanced DTG fingerprinting with appropriate standards can detect specific fillers at low concentrations, the additive's identity is still inferred from its decomposition pattern rather than from direct molecular measurement. Consequently, TGA serves as a foundational screening tool that must be complemented by



other techniques, such as elemental analysis or evolved gas spectroscopy, to identify the specific molecular composition of the residual mass or the additives present.

## 6.2. DSC for polymer additive analysis

**6.2.1. Fundamentals and limitations.** DSC is another common thermal characterization method for semicrystalline polymers. DSC measures the heat flow associated with phase transitions and chemical reactions as a function of temperature. In a DSC experiment, the difference in the heat flow between a sample and a reference is recorded as the temperature changes. The sample is placed in a sealed pan, and the excess energy required to heat (or cool) the sample, relative to an empty pan, is recorded. During the measurement, both the sample and the reference are heated at a constant rate. Since DSC operates under constant pressure, the heat flow is directly related to enthalpy changes by the following equation:

$$\frac{dq}{dt} = \frac{dH}{dt} \quad (1)$$

where  $\frac{dq}{dt}$  represents the heat flow and  $\frac{dH}{dt}$  represents the change in enthalpy. The following equation gives the heat flow difference between the sample and the reference.

$$\Delta \frac{dH}{dt} = \left( \frac{dH}{dt} \right)_{\text{sample}} - \left( \frac{dH}{dt} \right)_{\text{reference}} \quad (2)$$

Typically, DSC is used to determine the melting temperature ( $T_m$ ), crystallization temperature ( $T_c$ ), glass transition temperature ( $T_g$ ), and the corresponding enthalpy of these phase changes. The heat flow value can be either positive or negative based on the nature of the process. In an endothermic process, such as melting, heat is absorbed by the process. As a result, the value is positive. Conversely, in exothermic processes, such as crystallization or many cross-linking reactions, heat is released. In contrast, the glass transition is not associated with heat absorption or release but instead involves a change in heat capacity as the polymer transitions from a glass

to a rubbery state.<sup>141</sup> Crystallinity can be estimated by comparing the measured enthalpy of melting ( $\Delta H_m$ ) to the enthalpy of melting for a 100% crystalline polymer ( $\Delta H_m^0$ ), using the equation:

$$\% \text{ Crystallinity} = \left( \frac{\Delta H_m}{\Delta H_m^0} \right) \times 100\% \quad (3)$$

A simplified diagram of DSC, along with a representative DSC curve, is shown in Fig. 14.

In practice, DSC experiments are often carried out in a heat-cool-heat cycle. The first heating removes thermal history and processing effects (such as residual stress or incomplete crystallization), the controlled cooling step, and the second heating provides reproducible data on thermal transitions. Typical heating and cooling rates range from 5 to 20 °C min<sup>-1</sup>, depending on the sensitivity required, while sample sizes are usually 5–10 mg.

Like TGA, DSC detects the presence of copolymers or additives through shifts in thermal properties. Unlike TGA, which focuses on degradation and volatilization, DSC examines phenomena such as melting, glass transition, and crystallinity. DSC alone cannot be used to quantify the amount of an additive or the specific additive. Therefore, it is better to use DSC as a secondary validation characterization tool in identifying any polymer or additive.

**6.2.2. Recent advances and current trends.** While DSC is widely used to analyze the thermal behavior of polymers and polymer blends, it is not used for the direct detection and identification of unknown additives. However, there are a few studies that utilized DSC to follow the shift in thermal properties as a function of the loading of a polymer with a known additive. These studies illustrate that additive loading can be tracked by DSC after a proper calibration set is obtained. Hong *et al.* attempted to improve the crystallization and thermal stability of polyhydroxybutyrate (PHB) by adding polymeric carboxyl-terminated butadiene acrylonitrile rubber (CTBN) and biocompatible polyvinylpyrrolidone (PVP) as additives at con-

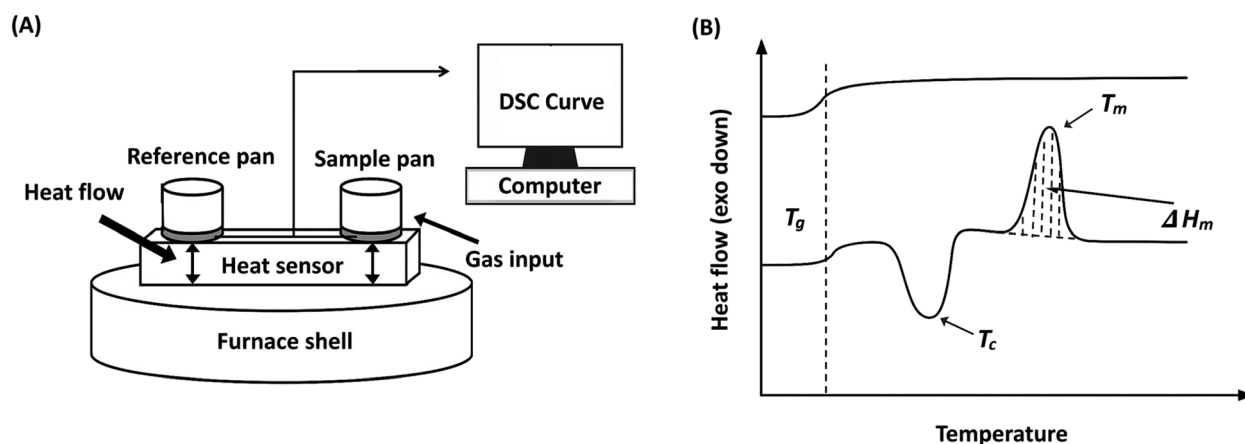


**Fig. 14** (A) Basic schematic of a DSC showing sample and reference pans with a heat sensor, (B) a representative DSC curve indicating glass transition ( $T_g$ ), crystallization ( $T_c$ ), and melting ( $T_m$ ) events.



centrations of 1–2 wt%.<sup>64</sup> The cooling DSC results showed that neat PHB crystallized slowly, with a broad exothermic peak and a low crystallization temperature ( $\sim 71$  °C). The addition of CTBN or PVP shifted crystallization to higher temperatures and produced narrower peaks, indicating faster crystallization. The additives also increased the crystallinity. In the second heating DSC curves, neat PHB showed two melting peaks at  $\sim 150.5$  °C and  $\sim 163.8$  °C. The addition of CTBN led to higher  $T_m$  values and PVP had an even stronger effect, producing the highest  $T_m$  values. Overall, both CTBN and PVP improved crystallization behavior, with PVP being the most effective additive.<sup>64</sup> This study demonstrates how DSC can be useful for evaluating the influence of additives on polymer crystallization and melting behavior and how it may be applied to track additive effects in polymer systems when the additives and their loadings are known.

In contrast to examining the crystallization and melting behavior of semicrystalline polymers, Rahman and Brazel utilized DSC to evaluate changes in the glass transition temperatures of poly (vinyl chloride) from traditional and ionic liquid (IL) plasticizers at 20 wt% loading.<sup>65</sup> They found a significant reduction in the glass transition temperatures of PVC when traditional plasticizers were present compared to IL plasticizers. However, differences among the plasticization effects of ILs were also evident: imidazolium-based ILs showed the least reduction in  $T_g$ , reflecting stronger secondary bonding and partial incompatibility compared to other ILs. Thus, DSC served as a sensitive tool to quantify plasticization and distinguish the relative efficiency of different additives through shifts in  $T_g$ .<sup>65</sup> This work suggests DSC could be used to infer the presence of compatibilizers that are used to increase the stability of polymers that do not blend. The addition of compatibilizers can result in additional peaks or glass transitions in the DSC results. An example is the study by Ferrarezi *et al.*<sup>63</sup> DSC results showed that PLA exhibited a glass transition near 83 °C with crystallinity ( $\sim 18\%$ ). Blending with thermoplastic starch (TPS) or polyethylene glycol (PEG) resulted in additional glass transitions, with blends generally presenting two  $T_g$  values: a lower  $T_g$  (1) associated with TPS or PEG and a higher  $T_g$  (2) associated with PLA. The detection of two distinct transitions indicated phase separation in most blends, except TPS/PEG, which behaved as a miscible system. The PLA/TPS blend showed a reduced  $T_g$  (2) compared to neat PLA due to the plasticizing effect of glycerol, while ternary PLA/TPS/PEG blends exhibited even lower  $T_g$  (2) values, confirming the combined plasticization effects of glycerol and PEG.<sup>63</sup> This study suggests that in the case of immiscible systems, the presence of additional  $T_g$  transitions may indicate the presence of additives.

The literature indicates that DSC serves as a powerful tool for monitoring phase behavior, yet it remains a fundamentally indirect and inferential method for additive analysis. As the discussed studies show, DSC does not directly detect or identify additives; instead, their presence is inferred from measurable shifts in crystallization kinetics, melting temperatures, or the appearance of secondary glass transitions. While these

thermal signatures are sensitive enough to distinguish the efficiency of different plasticizers or the compatibility of blends, their interpretation depends heavily on prior knowledge of the additive system and the availability of calibration data. Furthermore, because overlapping transitions and complex thermal histories can obscure these effects, DSC lacks the structural specificity required for independent identification. Consequently, DSC is best utilized as a comparative technique to assess the influence of known additives on polymer performance, requiring support from spectroscopic and chromatographic methods to resolve the chemical identities of the additives responsible for changes in phase behavior.

### 6.3. XRD for polymer additive analysis

**6.3.1. Fundamentals and limitations.** XRD is used to understand the crystallographic structure of a material. In an X-ray diffraction experiment, the sample is placed into the center of an instrument and illuminated with a beam of X-rays. A basic diagram of the method is provided in Fig. 15 (A). The X-ray source tube and the detector move in a synchronized motion. The X-rays generated (incident X-rays) get diffracted from the sample to the detector. The X-rays are diffracted based on the crystallographic arrangements of the atoms within the sample. Constructive or destructive interference between X-rays scattered from neighboring planes in the crystals, as shown in Fig. 15(B), results in peaks in the diffractogram. The diffracted X-rays received at different angles ( $2\theta$ ) of the sample are presented as a diffractogram, a plot of diffracted X-ray intensity *versus*  $2\theta$ . Bragg's law is utilized to determine the interplanar spacing of the crystal lattice, thereby elucidating the material's specific crystal structure, and is defined by the following equation:

$$n\lambda = 2d \sin(\theta) \quad (4)$$

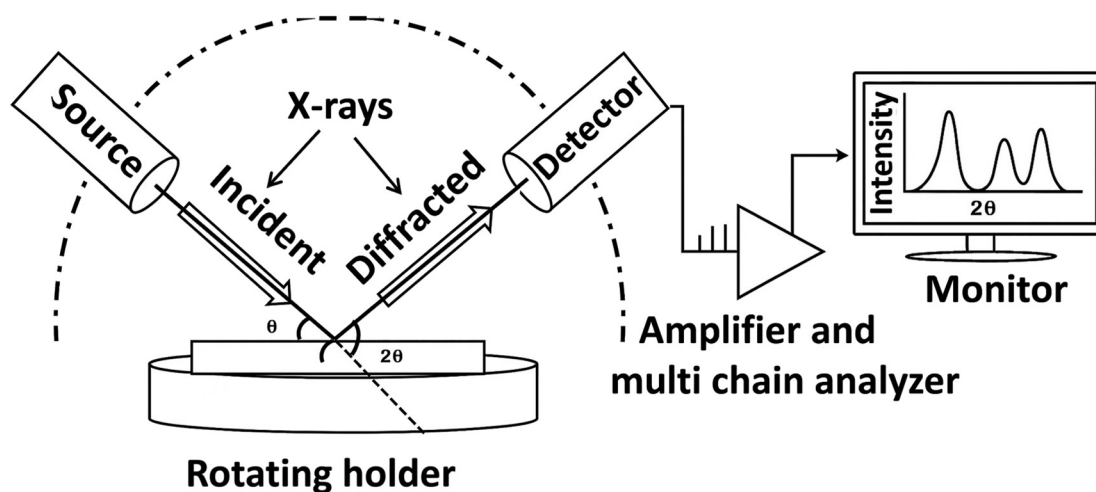
where  $n$  is the order of reflection,  $\lambda$  is the wavelength of the incident X-rays,  $d$  is the interplanar spacing between the crystallographic planes and  $\theta$  is the angle of incidence.

When additives are incorporated into a polymer matrix, they can influence the material's crystallinity, interplanar spacing, and overall molecular organization. Changes such as peak shifts, broadening, or intensity variations in the XRD diffractogram can indicate the presence of additives and reflect an altered crystal structure. Additionally, if the additives themselves are crystalline, they can contribute their own characteristic diffraction peaks to the XRD pattern. In this case, the additional diffraction peaks can be used to identify the additives themselves.

XRD requires careful sample preparation, and characterizing amorphous and weakly crystalline polymers using XRD is particularly challenging. This is because the diffraction patterns primarily arise from the crystalline regions in the sample, where atomic planes produce well-defined Bragg diffraction peaks. In contrast, amorphous regions lack long-range order and therefore produce broad humps instead of true diffraction peaks. Sample thickness also plays an important role,



(A)



(B)

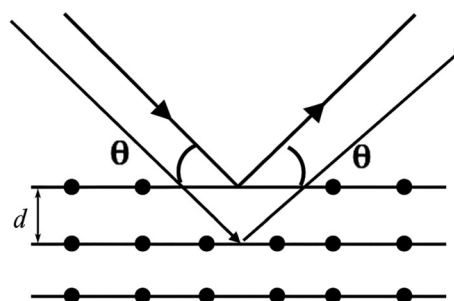


**Fig. 15** (A) Simplified schematic of an X-ray diffraction (XRD) instrument, showing the X-ray source, sample, detector, and resulting diffraction pattern; (B) illustration of Bragg's law, relating diffraction angle ( $\theta$ ) and interplanar spacing ( $d$ ).

as thicker samples tend to absorb more X-rays and minimize observed diffraction.<sup>142–144</sup> Thus, XRD can be used to monitor conformational changes only when the polymeric materials being analyzed are crystalline or semi-crystalline. For quantitative analysis, XRD can be used to estimate the relative concentration of additives in polymers by assessing changes in the polymer's degree of crystallinity. However, this method is not directly quantitative; it only offers an indirect, comparative measure based on how additives influence polymer crystallinity, and requires an understanding of which additives are present.

Conversely, if the additives are crystalline, their XRD peaks tend to be very weak relative to the intense peaks of the polymer matrix, making them difficult to identify. However, if the peaks are sufficiently distinct from the polymer background, various XRD analysis software can be used to compare experimental data with standard diffraction patterns from the ICDD (International Centre for Diffraction Data) PDF-4+ database or similar databases to identify these peaks. Compared to other characterization techniques, XRD has a poor limit of detection for additives within the sample. Thus, information provided by this technique needs to be coupled with other techniques to validate the findings.

**6.3.2. Recent advances and current trends.** There are limited reports in the literature on the use of XRD to detect additives in polymers. Papajani *et al.* showed the influence of additives on the crystallinity of LDPE by combining FTIR spectroscopy and XRD.<sup>66</sup> Experimental XRD diffractograms of seven LDPE samples (one pure LDPE with no additive, six recycled LDPE samples with different amounts of additives) confirmed that both pure and recycled materials were semi-crystalline, showing sharp peaks from crystalline regions and a broad hump from amorphous content. All LDPE samples displayed two characteristic polyethylene peaks at  $2\theta$  angles of  $21.73^\circ$  and  $24.18^\circ$ . Compound identification was performed by comparing the experimental XRD patterns of the recycled samples with reference spectra from the reference database using X'Pert HighScore Plus software. This analysis revealed the presence of crystalline UV stabilizer additives such as rutile ( $\text{TiO}_2$ ) and calcite ( $\text{CaCO}_3$ ) in the recycled materials.<sup>66</sup>

An example of the use of XRD for additive studies in amorphous polymer is the work by Deraman *et al.*<sup>67</sup> They studied the effect of plasticizers on the PVC-salt samples using XRD where PVC was blended with an added salt to form a polymer-salt complex, and then two plasticizers were introduced at known concentrations. The plasticizers used were ethylene car-



bonate (EC) and  $\text{Bu}_3\text{MeNTf}_2\text{N}$  (butyltrimethyl ammonium bis(trifluoromethylsulfonyl)imide). XRD was instrumental in revealing how varying plasticizer concentrations influenced the crystallinity of the PVC-salt samples. In both the EC and  $\text{Bu}_3\text{MeNTf}_2\text{N}$ -based systems, XRD patterns showed broad humps instead of sharp peaks, indicating predominantly amorphous structures. By analyzing the position and intensity of these amorphous humps, changes in crystallinity were evaluated. For example, in the EC system, increasing the plasticizer concentration from 5 to 15 wt% shifted the center of the hump from  $2\theta = 23^\circ$  to  $18^\circ$ , along with changes in intensity indicating increased amorphous character and disrupted crystalline order. Similarly, in the  $\text{Bu}_3\text{MeNTf}_2\text{N}$  system, changes in the  $2\theta$  position and relative intensity of the hump were used to quantify the additive content of the sample, which correlated with the known concentration.<sup>67</sup> The study conducted by Dankar *et al.* revealed that additives such as glycerol and lecithin influenced the crystallinity of potato puree by altering peak intensity.<sup>68</sup> Glycerol significantly reduced crystallinity, indicating substantial disruption of starch structure, while lecithin enhanced order at higher concentrations. These changes demonstrated that XRD effectively inferred the presence of additives in the polymer matrix.<sup>68</sup>

The literature indicates that XRD serves as a specialized structural probe for monitoring additive-induced changes in polymer crystallinity, yet its effectiveness is fundamentally tied to the physical state of the components. As the discussed studies show, XRD provides valuable data on the presence of crystalline additives—such as mineral pigments and stabilizers—and can infer the influence of plasticizers by tracking shifts in amorphous humps or peak intensities. However, a significant comparative conclusion emerges: the utility of XRD is primarily restricted to additives that either possess inherent crystallinity or significantly disrupt the polymer's semi-crystalline order. Because many organic additives are amorphous or present at concentrations below the technique's detection limits, they often remain invisible against the dominant amorphous halo of the host polymer. Consequently, XRD is best utilized as a complementary tool for structural assessment rather than a primary identification method. It requires support from molecular spectroscopy to characterize unknown or non-crystalline additive packages.

Physical and thermal analyses provide inferential evidence of the presence of an additive by monitoring changes in the host polymer's behavior. While these methods are non-definitive for structural identification, their ability to detect anomalies at low concentrations makes them indispensable screening tools. The roadmap (Section 8) utilizes these thermal and structural signatures to assist with screening for potential additive content when the polymer is known.

## 7. Evolved gas analysis for polymer additive analysis

Evolved gas analysis (EGA) is an analytical approach used to study the gases released by a material as it is heated, along

with the temperatures at which thermal decomposition or other chemical changes occur. In a typical EGA experiment, the sample is heated in a controlled manner while its mass loss is continuously monitored (thermogravimetry). As volatile compounds evolve, they are transferred directly to a suitable analyzer, such as a mass spectrometer or a FTIR spectrometer. These detectors provide complementary information: MS characterizes the molecular masses and fragmentation patterns of the gases, while FTIR spectroscopy identifies their functional groups. The combined thermal and analytical data yield a detailed profile of the material's composition and decomposition behavior.

### 7.1. Fundamentals and limitations

The way volatile products are generated from a polymer strongly influences analytical resolution, specificity, and applicability for additive identification. The primary gas-generation approaches are flash pyrolysis (Py), multi-shot pyrolysis (MPy), and thermogravimetric analysis (TGA). Py employs rapid heating—often to 500–800 °C within seconds—to break polymer chains and release volatile fragments. Thermogravimetric analysis (TGA) uses slow, controlled heating under a specified atmosphere to monitor real-time weight loss as gases evolve from a sample. Multi-shot pyrolysis bridges the gap between flash pyrolysis and TGA by applying a programmed sequence of discrete pyrolysis temperatures. The advantage of using TGA to produce the gaseous product is that the thermal degradation profile is simultaneously obtained, allowing specific compounds in the evolved gas to be correlated with degradation events observed in the TGA degradation profile. Coupling TGA to spectral detectors enables simultaneous thermal and chemical characterization of the volatiles produced during the TGA analysis. A simplified diagram of evolved gas analysis is shown in Fig. 16. For instance, TGA-MS transfers the evolved gases directly into a mass spectrometer, providing rapid, highly sensitive detection and allowing determination of molecular masses and fragmentation patterns. This makes TGA-MS particularly useful for detecting low-level or inorganic gaseous products, although the absence of chromatographic separation can lead to overlapping signals in

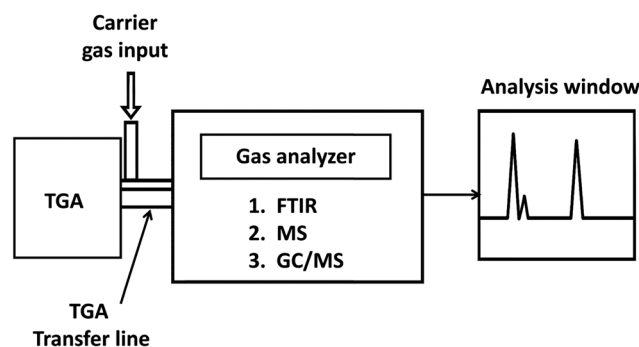


**Fig. 16** Basic schematic of evolved gas analysis (EGA), where gases released during TGA are transferred to spectral detectors such as FTIR, MS, or GC-MS for real-time analysis.



complex mixtures. In contrast, TGA-GC/MS introduces the evolved gases into a gas chromatograph prior to mass spectrometric detection, enabling correlation of each weight-loss event with well-resolved chromatographic peaks and associated mass spectra. These spectra can be compared against established reference databases, such as the NIST mass spectral library, to identify specific compounds. TGA-FTIR can likewise link mass-loss steps to infrared spectral features, providing direct information on the functional groups present in the released species. While TGA-GC/MS and TGA-MS approaches are powerful for mechanistic studies or pinpointing the precise temperatures at which additives volatilize, they are less commonly used for routine additive identification due to broader peaks from slower heating rates and the limited availability of libraries for TGA-derived products compared to pyrolysis GC/MS. TGA-FTIR, on the other hand, serves as an alternative for functional group assignment without chromatographic separation. It is quite common due to its relatively quick acquisition times and breadth of applications. It is often used to characterize polymers and inorganic materials, with about 50% of applications focused on these two classes.<sup>145,146</sup> The off-gas produced during heating can lead to convoluted signals in the TGA data.<sup>147</sup> The Gram-Schmidt plot contains all of the FTIR spectral information, showing signal intensity *versus* temperature (or time).<sup>148</sup> From this, major thermal events can be identified and analyzed by examining the associated FTIR spectral data over a given temperature interval or time window. However, there are a few significant limitations related to TGA-FTIR. The FTIR spectroscopy must be done as quickly as possible to avoid secondary reactions in the gas phase during transfer. Moreover, there are often significant temperature differences between the furnace and transfer lines, which can lead to condensation and, as a result, clogging by higher-molecular-weight compounds. Aside from the technical limitations, coupled instrumentation is not nearly as common as merely having a TGA or FTIR spectrometer available.

## 7.2. Recent advances and current trends

The study by Fedelich *et al.* utilized TGA-MS to quantify a small number of known additives in a polymer.<sup>69</sup> They spiked butyl rubber (BR, 130 mg) with methyl salicylate (0.5, 1, and 5  $\mu\text{L}$ ). Using these samples, TGA-MS was performed by heating the rubber up to 300  $^{\circ}\text{C}$  while monitoring both the mass loss and the ion signals by MS. Although the TGA curves of low-concentration samples closely resembled that of pure rubber, the MS provided enhanced sensitivity, showing a clear ion signal corresponding to the release of methyl salicylate. By integrating this signal and comparing it to calibration curves, the researchers quantified the additive in the microgram range and determined a detection limit of 0.5  $\mu\text{L}$ .<sup>69</sup> This demonstrates that TGA-MS can identify and quantify trace volatile additives in polymers even when TGA alone cannot resolve them.

Tomiak *et al.* used TGA-GC/MS to determine changes in the decomposition of polyamide 6 mixed with expandable graphite

or a mixture of aluminum diethylphosphinate (ALPi) and melamine polyphosphate (MPP).<sup>71</sup> They analyzed the gaseous products at two heating rates, 20  $\text{K min}^{-1}$  and 100  $\text{K min}^{-1}$ , and found a difference in peak-area percentages. A slight reduction in the elution temperature of certain gaseous products was also noted when PA6 was mixed with ALPi/MPP.<sup>71</sup> Yousef *et al.* added carbon black to glass fiber-reinforced polymers to assess the pyrolysis recyclability of the composites.<sup>70</sup> They found that phenol products were abundant during pyrolysis and suggested that a high phenol content would make the material viable for recycling for energy and recovering the glass fibers at low temperatures.<sup>70</sup>

These studies show that TGA-GC/MS is a facile method to determine the gaseous components of polymer degradation steps. However, it is quite difficult to determine the specific additives in polymers based solely upon TGA-GC/MS analysis because many additives degrade simultaneously with the polymer matrix, producing overlapping signals that complicate interpretation. Another related approach, TGA-FTIR, has also been explored for additive detection. While it shares many of the same advantages of real-time evolved gas monitoring, its application to polymer additives remains relatively limited. One notable exception is a comprehensive polymer additive identification study reported by Cuthbertson *et al.*, using various techniques, including TGA-FTIR.<sup>52</sup> They analyzed 21 different polymers from various classes using TGA-FTIR to detect and identify additives. They were able to identify monomers, typical degradation products, and additives in the evolved gases. For instance, they found alkanes in PE; benzene, hydrogen chloride, and 1-chlorooctane in PVC; styrene in PS; acetic acid in PVOH, EVOH, and EVA; and methyl methacrylate in PMMA. They identified butylated hydroxytoluene (BHT) within one of their PE samples, which is commonly used as an antioxidant to prevent degradation of polyolefins by UV or thermal mechanisms. One of the PVC samples evaluated was determined to contain 5-norbornene-2,3-dicarboxylic anhydride (NBDCA), a compound used primarily as a processing aid. They detected the presence of pentane in one PS sample and later confirmed from the vendor the use of pentane as a blowing agent.<sup>52</sup>

Evolved-gas analysis (EGA) provides high sensitivity for detecting volatile degradation products and trace additives, particularly when mass-loss curves alone are insufficient. However, the literature indicates that EGA remains less widespread than techniques such as Py-GC/MS for identifying unknown additive packages. This disparity stems from a significant analytical bottleneck: in complex polymer systems, many additives and polymer matrices decompose within similar temperature ranges. Such simultaneous decomposition produces overlapping signals that are difficult to interpret without the chromatographic separation provided by Py-GC/MS. Furthermore, the broader adoption of EGA is currently constrained by systemic factors, including high instrumentation costs, the requirement for specialized workflows, and a lack of comprehensive evolved-gas spectral libraries dedicated to polymer additives. Consequently, while EGA is a powerful



tool for monitoring thermal behavior, its role in definitive additive identification is often relegated to a complementary rather than a primary technique.

Evolved gas analysis bridges the gap between thermal behavior and chemical identity by monitoring degradation products in real-time. Despite challenges with signal overlap and library availability, it provides a unique dimension of data for volatile components. This technique is integrated into the roadmap (Section 8) as a specialized path for characterizing additives that are otherwise inaccessible *via* traditional extraction methods.

## 8. Proposed roadmap

The analytical roadmap for evaluating additives in a polymer sample is rarely a “one-size-fits-all” approach; instead, it must be tailored to the specific level of prior knowledge of the sample’s composition. In practice, researchers, analysts, quality engineers, and regulatory specialists typically encounter one of four scenarios, each requiring a distinct entry point into the analytical pathway:

- Case 1: Known polymer and known additive. The analyst possesses significant prior knowledge of the material’s composition. The primary objective is to determine the additive’s relative concentration for quality control or performance verification.

- Case 2: Known polymer with unknown additive presence. The matrix has been identified, but it is unclear whether additives were introduced intentionally or accidentally. This is common when troubleshooting production defects or evaluating “equivalent” resin grades from new suppliers.

- Case 3: Unknown polymer and unknown additives. This represents a “blind” analysis in which both the host matrix and additives must be determined from scratch, as in competitor product deconstruction or environmental microplastics research.

- Case 4: Unknown polymer with a suspected or detected additive. This occurs when a specific additive signal, such as the white opacity of TiO<sub>2</sub>, a characteristic leaching product, or a distinct odor, is observed before the host matrix is identified.

As outlined in Fig. 17, these starting points determine the sequence of screening and characterization techniques employed. While the entry points differ, the workflows are intrinsically linked: the effort in Cases 3 and 4 includes analysis to determine the polymer type, while Cases 2 and 3 utilize techniques to detect and identify additives. Ultimately, all pathways converge on Case 1 once the chemical identities are established, enabling rigorous quantification.

Case 1 exhibits the highest level of certainty and is frequently a starting point for analysis in polymer production, compounding, and converting operations. Because chemical identities are established, the analytical objective is focused entirely on quantification. For additives such as antioxidants (AO), UV stabilizers (UVS), plasticizers (PL), processing aids

(PA), slip additives (SA), compatibilizers (CMB), and impact modifiers (IM), selective solvent extraction followed by GC or HPLC enables specific quantification using calibration curves generated from known reference standards. When additives contain distinctive elemental markers such as phosphorus-based flame retardants (FR), metal-containing heat stabilizers (HS), inorganic additives (IA), or mineral fillers (FL), the workflow preferentially routes to ICP-based techniques or CHNS for elemental quantification. Spectroscopic techniques such as FTIR or NMR are incorporated only when additives exhibit strong, isolated signals that enable reliable calibration. In contrast, Py/TGA-GC methods serve as complementary routes for non-extractable or thermally unstable additives.

Case 2 prioritizes detection and chemical classification before attempting concentration measurements. The workflow begins with non-targeted spectroscopic screening using FTIR, Raman, and NMR. Because the polymer background is known, deviations from expected polymer signatures can be attributed to additives, enabling class-level inference for organic additives. When spectroscopic contrast is insufficient due to low loadings or spectral overlap, thermal and evolved-gas techniques (Py-GC/MS, TGA-FTIR) are used to provide characteristic fragments of FR, HS, IM, and other additives. Elemental screening can be used to reveal heteroatoms not present in the base polymer. Once the additive chemistry is narrowed, the scenario reverts to the Case 1 framework for quantification.

Case 3 is the most analytically challenging scenario, often involving materials that contain degraded polymers and additive byproducts. Because no chemical baseline exists, the strategy must first establish polymer identity. The effort begins with FTIR, Raman, and NMR spectroscopy to identify the polymer family and detect copolymers or blends. Property-based techniques (TGA, DSC, and XRD) can be integrated at this stage to differentiate polymer classes based on thermal behavior and crystallinity. Py-GC/MS and evolved gas analysis provide complementary polymer fingerprints while simultaneously revealing additive-related pyrolysis products. Once the polymer is identified, the system reverts to a Case 2 scenario to characterize the specific additive package.

Case 4 is triggered when additive-specific markers are identified during initial handling or preliminary screening. Examples include visual detection of inorganic fillers such as TiO<sub>2</sub>, identification of phosphorus-based flame retardants during elemental screening, and observation of additive migration into a surrounding medium. In this pathway, identifying the polymer matrix is the immediate priority to provide a quantitative baseline. By establishing the polymer identity through spectroscopic and thermal techniques, the analyst can define the matrix’s contribution to spectroscopic and elemental analysis signals. Pyrolysis-based techniques (Py-GC/MS) are especially effective here, as they simultaneously confirm the polymer’s pyrolysis fragments and the additive’s marker compounds. Once the matrix is identified and its interference potential is understood, the workflow converges into Case 1 for final quantification.





Fig. 17 Flowchart outlining the roadmap for detection, identification, and quantification of polymer additives.

Ultimately, the choice of an analytical entry point is a strategic decision based on the balance of known and unknown variables within a sample. While the initial stages of each case differ, prioritizing either rapid quantification, “blind” screening, or matrix identification, the overarching goal remains a complete chemical and physical characterization. By following this tiered approach, the analyst avoids the inefficiencies of redundant testing and ensures that the final quantification is grounded in an accurate understanding of the polymer matrix. Whether driven by industrial quality control, competitive

benchmarking, or regulatory necessity, this integrated workflow provides a robust framework for navigating the inherent complexity of modern polymer-additive analysis.

## 9. Conclusion

Growing industrial demands for high-performance polymers, combined with increasing environmental pressures from global sustainability goals and recycling mandates, have made



accurate additive analysis more critical than ever. As this review illustrates, the necessity for additive tracking spans the entire material lifecycle, beginning with polymer production, where inhibitors are used to control synthesis. During compounding operations, primary and secondary antioxidants must be precisely dosed to protect the resin from thermal stress, while converting operations introduce pigments and stabilizers as the polymer is shaped into final products. In both cases, quality assurance requires the careful monitoring of additive content and distribution. Beyond manufacturing, analytical methods are essential for determining the life span of materials by monitoring the leaching or degradation of these additives during service.

The analytical challenge reaches its peak at the end-of-life stage, where the detection of restricted legacy additives is vital for technical traceability and the forensic analysis of environmental microplastics. Furthermore, the precise measurement of residual additives in reclaimed polymers is essential for determining the safety, quality, and potential for valorization of recycled streams. To navigate these complexities, our proposed roadmap provides a framework for selecting appropriate techniques based on the analysis's specific goal and the initial state of knowledge about the material. This strategic framework is structured around four primary scenarios, ranging from well-defined industrial formulations to completely unknown environmental fragments. By using the roadmap, researchers can determine whether to employ inferential screening tools such as TGA and DSC for rapid assessment or more resource-intensive molecular methods such as GC-MS and NMR spectroscopy for definitive characterization. Ultimately, the systematic application of these methodologies supports the development of safer materials and the valorization of reclaimed plastics, providing a foundation for a more transparent and sustainable polymer value chain.

## Author contributions

Tanmay Rahman: writing – original draft, writing – review & editing, preparation of figures. Daniel Meadows: writing – review & editing, preparation of figures. Ke Zhan: writing – review & editing, preparation of figures. Harrish Kumar Senthil Kumar: writing – review & editing, preparation of figures. Marshall Smith: writing – review & editing, preparation of figures. Virginia A. Davis: writing – review & editing, supervision, funding acquisition. Bryan S. Beckingham: writing – review & editing, supervision, funding acquisition. Yucheng Peng: writing – review & editing, supervision, funding acquisition. Edward Davis: writing – review & editing, supervision, funding acquisition, conceptualization.

## Conflicts of interest

The authors declare no competing financial interest.

## Data availability

No primary research results, software or code have been included and no new data were generated or analysed as part of this review.

## Acknowledgements

The authors are grateful for the financial support provided by NSF #2132093 and NIST #60NANB24D018. The authors thank Zachary Bradford for drawing all chemical structures displayed in this work.

## References

- 1 J. Brady, T. Dürig, P. Lee and J.-X. Li, in *Developing solid oral dosage forms*, Elsevier, 2017, pp. 181–223.
- 2 C. A. Harper, *Handbook of plastics technologies: the complete guide to properties and performance*, McGraw-Hill, 2006.
- 3 K. Zhan, D. Meadows, L. Levy, R. Hou, T. Rahman, V. Davis, E. Davis, B. S. Beckingham, B. Via and T. Elder, *Polym. Degrad. Stab.*, 2024, **222**, 110710.
- 4 R. Pfaendner, in *Handbook of Polymer Synthesis, Characterization, and Processing*, ed. E. Saldívar-Guerra and E. Vivaldo-Lima, John Wiley & Sons, Inc., 2013, ch. 11, pp. 225–247.
- 5 J. George, M. S. Sreekala and S. Thomas, *Polym. Eng. Sci.*, 2001, **41**, 1471–1485.
- 6 V. Marturano, P. Cerruti and V. Ambrogi, *Phys. Sci. Rev.*, 2017, **2**, 20170138.
- 7 M. Ahmad, D. Shukla, Y. Zhu and O. D. Velev, *ACS Appl. Mater. Interfaces*, 2025, **17**, 17316–17329.
- 8 U. Heudorf, V. Mersch-Sundermann and J. Angerer, *Int. J. Hyg. Environ. Health*, 2007, **210**, 623–634.
- 9 Y. Guo and K. Kannan, *Anal. Bioanal. Chem.*, 2012, **404**, 2539–2554.
- 10 G. Song, J. Tao, L. Cui, S. Ma, Q. Lv, H. Chen, X. Liu, Y. Yang and D. Chen, *Environ. Sci. Technol. Lett.*, 2024, **11**, 23–28.
- 11 A. D. Godwin, in *Applied Plastics Engineering Handbook*, ed. M. Kutz, Elsevier, 3rd edn, 2024, ch. 26, pp. 595–618.
- 12 Plasticizers Market by type (phthalate and non-phthalate), Application (Floorings & Wall Coverings, Films & Sheets, Coated Fabrics, Wires & Cables, Consumer Goods), and Region (North America, Europe, Middle East, and Africa)-Global, *Forecast to 2027*, <https://www.marketsandmarkets.com/Market-Reports/plasticizers-market-688.html> (accessed 23 December, 2025).
- 13 E. Kriek, *Biochim. Biophys. Acta, Rev. Cancer*, 1974, **355**, 177–203.
- 14 X. Meng, W. Chen, Z. Xin and C. Wu, *J. Vinyl Addit. Technol.*, 2018, **24**, 124–129.
- 15 K. Schwetlick, *Pure Appl. Chem.*, 1983, **55**, 1629–1636.



- 16 J. Ngunjiri, P. Michaeleen and S. Rahul, *Microsc. Microanal.*, 2021, **27**, 2010–2010.
- 17 R. Höfer, in *Polymer Science: A Comprehensive Reference*, ed. K. Matyjaszewski and M. Möller, Elsevier, 2012, vol. 10, ch. 10.21, pp. 369–381.
- 18 C. Ye, Z. Liu, J. Li, Y. Ni, Z. Xin and S. Zhao, *J. Polym. Res.*, 2023, **30**, 7.
- 19 R. Li, S. Xu, J. Xu, T. Pan, B. Sun and L. Dang, *Polymers*, 2023, **15**, 2575.
- 20 J. G. Drobny, in *Handbook of Thermoplastic Elastomers*, ed. J. G. Drobny, William Andrew, 2nd edn, 2014, ch. 3, pp. 17–32.
- 21 C. A. De Wit, *Chemosphere*, 2002, **46**, 583–624.
- 22 S. V. Levchik and E. D. Weil, *J. Fire Sci.*, 2006, **24**, 345–364.
- 23 C. A. Willkie and A. B. Morgan, *Fire Retardancy of Polymeric Materials*, CRC Press, Boca Raton, 3rd edn, 2024.
- 24 E. Yousif and R. Haddad, *SpringerPlus*, 2013, **2**, 398.
- 25 P. Gijnsman, J. Hennekens and D. Tummers, *Polym. Degrad. Stab.*, 1993, **39**, 225–233.
- 26 D. Lala and J. F. Rabek, *Polym. Degrad. Stab.*, 1981, **3**, 383–396.
- 27 S. Kemmlein, D. Herzke and R. J. Law, *J. Chromatogr. A*, 2009, **1216**, 320–333.
- 28 P. Fauser, K. Vorkamp and J. Strand, *Mar. Pollut. Bull.*, 2022, **177**, 113467.
- 29 Y. Liu, M. Ahmad, R. A. Venditti, O. D. Velez and Y. Zhu, *Adv. Electron. Mater.*, 2024, **10**, 2300792.
- 30 R. Valand, S. Tanna, G. Lawson and L. Bengtström, *Food Addit. Contam., Part A*, 2020, **37**, 19–38.
- 31 J. Schmidt, M. Haave and W. Wang, *RSC Adv.*, 2025, **15**, 13041–13052.
- 32 N. Singh, B. Mann, R. Sharma, A. Verma, N. R. Panjagari and K. Gandhi, *Food Packag. Shelf Life*, 2022, **34**, 100975.
- 33 L. Bernard, D. Bourdeaux, B. Pereira, N. Azaroual, C. Barthélémy, C. Breyse, P. Chennell, R. Cuff, T. Dine, T. Eljezi, F. Feutry, S. Genay, N. Kambia, M. Lecoœur, M. Masse, P. Odou, T. Radaniel, N. Simon, C. Vaccher, C. Verlhac, M. Yessaad, B. Décaudin and V. Sautou, *Talanta*, 2017, **162**, 604–611.
- 34 C. Zeddami and N. Belhaneche-Bensemra, *Int. J. Polym. Mater.*, 2010, **59**, 318–329.
- 35 L. A. Agustina, Y. D. Lestari, A. A. Adhinanda, M. N. Ariesta, J. Choi, Y. P. Prananto and R. Febriani, *Acta Chim. Asiana*, 2024, **7**, 366–376.
- 36 Q. Li, Y. Tang, Z. Yan and P. Zhang, *Spectrochim. Acta, Part A*, 2017, **180**, 154–160.
- 37 T. Nørbygaard and R. W. Berg, *Appl. Spectrosc.*, 2004, **58**, 410–413.
- 38 R. W. Berg and A. D. Otero, *Vib. Spectrosc.*, 2006, **42**, 222–225.
- 39 J. Ehret-Henry, J. Bouquant, D. Scholler, R. Klinck and A. Feigenbaum, *Food Addit. Contam.*, 1992, **9**, 303–314.
- 40 F. Coelho, L. F. Vieira, R. Benavides, M. M. d. S. Paula, A. M. Bernardin, R. F. Magnago and L. d. Silva, *Int. Polym. Process.*, 2015, **30**, 574–584.
- 41 F. P. Miknis and K. P. Thomas, *Road Mater. Pavement Des.*, 2008, **9**, 59–72.
- 42 E. Zygadło-Monikowska, Z. Florjańczyk, A. Tomaszewska, M. Pawlicka, N. Langwald, R. Kovarsky, H. Mazor, D. Golodnitsky and E. Peled, *Electrochim. Acta*, 2007, **53**, 1481–1489.
- 43 K. V. Alexeeva and L. S. Solomatina, *J. Chromatogr. A*, 1986, **364**, 105–112.
- 44 J. W. Sinclair, L. Schall and N. T. Crabb, *J. Chromatogr. Sci.*, 1980, **18**, 30–34.
- 45 P. Perlstein and P. Orme, *J. Chromatogr. A*, 1985, **325**, 87–93.
- 46 F. C.-Y. Wang and A. D. Burleson, *J. Chromatogr. A*, 1999, **833**, 111–119.
- 47 J. C. J. Bart, *J. Anal. Appl. Pyrolysis*, 2001, **58–59**, 3–28.
- 48 P. G. Demertzis and R. Franz, *Food Addit. Contam.*, 1998, **15**, 93–99.
- 49 H. El Mansouri, N. Yagoubi and D. Ferrier, *Chromatographia*, 1998, **48**, 491–496.
- 50 B. Li, Z.-W. Wang, Q.-B. Lin, C.-Y. Hu, Q.-Z. Su and Y.-M. Wu, *J. Chromatogr. Sci.*, 2014, **53**, 1026–1035.
- 51 M. Thilén and R. Shishoo, *J. Appl. Polym. Sci.*, 2000, **76**, 938–946.
- 52 A. A. Cuthbertson, C. Lincoln, J. Miscall, L. M. Stanley, A. K. Maurya, A. S. Asundi, C. J. Tassone, N. A. Rorrer and G. T. Beckham, *Green Chem.*, 2024, **26**, 7067–7090.
- 53 H. Liang, D. Rodrigue and J. Brisson, *J. Appl. Polym. Sci.*, 2015, **132**, 42692.
- 54 Y. Hu, D. M. Stevens, S. Man, R. M. Crist and J. D. Clogston, *Drug Delivery Transl. Res.*, 2019, **9**, 1057–1066.
- 55 J. S. F. Pereira, C. L. Knorr, L. S. F. Pereira, D. P. Moraes, J. N. G. Paniz, E. M. M. Flores and G. Knapp, *J. Anal. At. Spectrom.*, 2011, **26**, 1849.
- 56 M. Hemmerlin, J. M. Mermet, M. Bertucci and P. Zydowicz, *Spectrochim. Acta, Part B*, 1997, **52**, 421–430.
- 57 H. Dvir, M. Goldraich, M. Gottlieb, S. Daren and J. Lopez Cuesta, *Polym. Degrad. Stab.*, 2001, **74**, 465–474.
- 58 R. D. Holbrook, J. M. Davis, K. C. K. Scott and C. Szakal, *J. Microsc.*, 2012, **246**, 143–152.
- 59 E. Fries, J. H. Dekiff, J. Willmeyer, M.-T. Nuelle, M. Ebert and D. Remy, *Environ. Sci.: Processes Impacts*, 2013, **15**, 1949–1956.
- 60 S. Won, K.-H. Ko, C.-J. Park, L.-R. Cho and Y.-H. Huh, *J. Adv. Prosthodont.*, 2022, **14**, 315.
- 61 K. Sałasińska, M. Borucka, M. Celiński, A. Gajek, W. Zatorski, K. Mizera, M. Leszczyńska and J. Ryszkowska, *Adv. Polym. Technol.*, 2017, **37**, 2394–2410.
- 62 D. Losic, F. Farivar, P. L. Yap and A. Karami, *Anal. Chem.*, 2021, **93**, 11859–11867.
- 63 M. M. F. Ferrarezi, M. de Oliveira Taipina, L. C. Escobar da Silva and M. d. C. Gonçalves, *J. Polym. Environ.*, 2012, **21**, 151–159.
- 64 S.-G. Hong, T.-K. Gau and S.-C. Huang, *J. Therm. Anal. Calorim.*, 2010, **103**, 967–975.



- 65 M. Rahman and C. S. Brazel, *Polym. Degrad. Stab.*, 2006, **91**, 3371–3382.
- 66 B. Papajani, E. Vataj, A. Hasımi and A. Sinanaj, in Published in part at RAD Conf. Proc., 2018, vol. 3, pp. 236–240.
- 67 S. K. Deraman, N. A. Tajuddin and H. Hanibah, *Sci. Lett.*, 2024, **18**, 78–91.
- 68 I. Dankar, A. Haddarah, F. E. L. Omar, M. Pujolà and F. Sepulcre, *Food Chem.*, 2018, **260**, 7–12.
- 69 N. Fedelich, *Evolved Gas Analysis Hyphenated Techniques*, Hanser Publishers, Munich, Germany, 2019.
- 70 S. Yousef, J. Eimontas, N. Striūgas and M. A. Abdelnaby, *Energy*, 2021, **233**, 121167.
- 71 F. Tomiak, A. Schoeffel, K. Rathberger and D. Drummer, *Polymers*, 2021, **13**, 2712.
- 72 Analytical Resolution vs. Detection Limit, <https://www.eag.com/wp-content/uploads/2016/11/M-006916-Bubble-Chart.pdf>, (accessed 23 December, 2025).
- 73 J. D. Schuttlefield and V. H. Grassian, *J. Chem. Educ.*, 2008, **85**, 279.
- 74 G.-L. Liu and S. G. Kazarian, *Analyst*, 2022, **147**, 1777–1797.
- 75 C. Berthomieu and R. Hienerwadel, *Photosynth. Res.*, 2009, **101**, 157–170.
- 76 K. Vrieze, *Recl. Trav. Chim. Pays-Bas*, 1991, **110**, 97–97.
- 77 A. Gonzalez, S. Garrigues, M. De La Guardia and S. Armenta, *Anal. Methods*, 2011, **3**, 43–52.
- 78 L. Lux, Y. Phal, P.-H. Hsieh and R. Bhargava, *Appl. Spectrosc.*, 2022, **76**, 105–117.
- 79 J. C. J. Bart, *Plastics Additives: Advanced Industrial Analysis*, IOS Press, 2006.
- 80 P. Griffiths and J. M. Chalmers, *Handbook of Vibrational Spectroscopy*, John Wiley & Sons, Ltd, 2006.
- 81 R. S. Das and Y. K. Agrawal, *Vib. Spectrosc.*, 2011, **57**, 163–176.
- 82 G. S. Bumbrah and R. M. Sharma, *Egy. J. Forensic Sci.*, 2016, **6**, 209–215.
- 83 A. Orlando, F. Franceschini, C. Muscas, S. Pidkova, M. Bartoli, M. Rovere and A. Tagliaferro, *Chemosensors*, 2021, **9**, 262.
- 84 A. Klisińska-Kopacz, B. Łydzba-Kopczyńska, M. Czarnecka, T. Koźlecki, J. del Hoyo Méendez, A. Mendys, A. Kłosowska-Klechowska, M. Obarzanowski and P. Frączek, *J. Raman Spectrosc.*, 2019, **50**, 213–221.
- 85 D. O. Hummel, *Atlas of Plastics Additives Analysis by Spectroscopic Methods*, Springer Berlin, Heidelberg, Germany, 1st edn, 2002.
- 86 G. J. Martin, M. L. Martin and J.-P. Gouesnard, *15N-NMR Spectroscopy (NMR Basic Principles and Progress)*, Springer-Verlag, Berlin, Heidelberg, ed. P. Diehl, 1989, pp. 1–69.
- 87 F. Hammerath, *Magnetism and Superconductivity in Iron-based Superconductors as Probed by Nuclear Magnetic Resonance*, Vieweg+Teubner Verlag Wiesbaden, 2012.
- 88 H. Günther, *NMR spectroscopy: basic principles, concepts and applications in chemistry*, John Wiley & Sons, 2013.
- 89 M. D. Reily and J. C. Lindon, *Metabonomics Toxic. Assess.*, 2005, 75–104.
- 90 I. Y. Slonim, *The NMR of polymers*, Springer Science & Business Media, 2012.
- 91 S. B. Chakrapani, M. J. Minkler and B. S. Beckingham, *Analyst*, 2019, **144**, 1679–1686.
- 92 S. B. Chakrapani, PhD thesis, Auburn University, 2019.
- 93 H. K. Senthil Kumar, Y. Noh, A. L. Bachmann and B. S. Beckingham, *Magn. Reson. Chem.*, 2024, **62**, 619–628.
- 94 H. Kessler, M. Gehrke and C. Griesinger, *Angew. Chem., Int. Ed. Engl.*, 1988, **27**, 490–536.
- 95 D. A. Meadows, H. K. S. Kumar, E. W. Davis, B. S. Beckingham and V. A. Davis, *Polym. Degrad. Stab.*, 2025, **232**, 111099.
- 96 C. B. Crawford and B. Quinn, in *Microplastic Pollutants*, ed. C. B. Crawford and B. Quinn, Elsevier, 2017, ch. 10, pp. 219–267.
- 97 R. Evers, PhD thesis, University of Portsmouth, 2014.
- 98 J. P. Dworzanski, L. Berwald, W. H. McClennen and H. L. C. Meuzelaar, *J. Anal. Appl. Pyrolysis*, 1991, **21**, 221–232.
- 99 T. Mitsui, M. Hida and Y. Fujimura, *J. Anal. Appl. Pyrolysis*, 1995, **32**, 205–212.
- 100 R. Milina, *J. Anal. Appl. Pyrolysis*, 1981, **3**, 179–183.
- 101 H. Nakagawa, S. Tsuge and K. Murakami, *J. Anal. Appl. Pyrolysis*, 1986, **10**, 31–40.
- 102 T. P. Wampler, *Applied Pyrolysis Handbook*, CRC Press, Boca Raton, 2006.
- 103 O. D. Sparkman, Z. Penton and F. G. Kitson, *Gas chromatography and mass spectrometry: a practical guide*, Academic press, 2011.
- 104 S. Mao, S. Tsuge, H. Ohtani, S. Uchijima and A. Kiyokawa, *Polymer*, 1998, **39**, 143–149.
- 105 F. C.-Y. Wang, *J. Chromatogr. A*, 2000, **883**, 199–210.
- 106 C. M. Rochman, *Marine anthropogenic litter*, 2015, pp. 117–140.
- 107 M. Herrera, G. Matuschek and A. Kettrup, *J. Anal. Appl. Pyrolysis*, 2003, **70**, 35–42.
- 108 S. H. d. l. Torre, in *Recent Perspectives in Pyrolysis Research*, ed. M. Bartoli and M. Giorcelli, IntechOpen, London, UK, 2022, ch. 15.
- 109 L. Hermabessiere, J. Receveur, C. Himber, D. Mazurais, A. Huvet, F. Lagarde, C. Lambert, I. Paul-Pont, A. Dehaut and R. Jezequel, *Sci. Total Environ.*, 2020, **749**, 141651.
- 110 B. Prathap, A. Dey, P. Johnson and P. Arthanariswaran, *Int. J. Novel Trends Pharm. Sci.*, 2013, **3**, 15–23.
- 111 V. Gupta, A. D. K. J. Jain, N. Gill and K. Gupta, *Int. Res. J. Pharm. Appl. Sci.*, 2012, **2**, 17–25.
- 112 B. K. Sharma, *Instrumental Methods of Chemical Analysis*, Krishna Prakashan, Meerut, India, 1981.
- 113 J. Gilbert, M. J. Shepherd, J. R. Startin and M. A. Wallwork, *J. Chromatogr. A*, 1982, **237**, 249–261.
- 114 M. Bird, C. Keitel and W. Meredith, in *Biochar: A Guide to Analytical Methods*, ed. B. Singh, M. Camps-Arbestain and J. Lehmann, CSIRO Publishing, Clayton South, Australia, 2017, pp. 39–50.



- 115 Analytical Methods Committee, Evaluation of analytical instrumentation. Part XIX. CHNS elemental analysers, *Accredit. Qual. Assur.*, 2006, **11**, 569–576.
- 116 V. P. Fadeeva, V. D. Tikhova and O. N. Nikulicheva, *J. Anal. Chem.*, 2008, **63**, 1094–1106.
- 117 R. F. André, J. Brandt, J. Schmidt, N. López-Salas, M. Odziomek and M. Antonietti, *Carbon*, 2024, **223**, 118946.
- 118 N. Z. Habib, I. Kamaruddin, I. M. Tan and M. Napiyah, in Presented in part at 7th RILEM International Conference on Cracking in Pavements, Delft University of Technology, The Netherlands, June 2012.
- 119 Y. Jia, J. Li, Y. Wang, J. Jin and H. Liu, *Prog. Org. Coat.*, 2021, **156**, 106249.
- 120 J. W. Olesik, *Anal. Chem.*, 1991, **63**, 12A–21A.
- 121 S. R. Khan, B. Sharma, P. A. Chawla and R. Bhatia, *Food Anal. Methods*, 2022, **15**, 666–688.
- 122 G. Tyler and J. Yvon, *ICP Optical Emission Spectroscopy Technical Note*, 1995, vol. 5.
- 123 P. W. J. M. Boumans and N. W. Barnett, *Anal. Chim. Acta*, 1987, **201**, 365.
- 124 P. K. Booth and C. W. McLeod, *Microchim. Acta*, 1989, **99**, 283–289.
- 125 J. Marshall, J. Franks, I. Abell and C. Tye, *J. Anal. At. Spectrom.*, 1991, **6**, 145–150.
- 126 D. R. Anderson, C. W. McLeod and T. A. Smith, *J. Anal. At. Spectrom.*, 1994, **9**, 67–72.
- 127 P. J. Fordham, J. W. Gramshaw, L. Castle, H. M. Crews, D. Thompson, S. J. Parry and E. McCurdy, *J. Anal. At. Spectrom.*, 1995, **10**, 303–309.
- 128 E. M. M. Flores, P. A. Mello, S. R. Krzyzaniak, V. H. Cauduro and R. S. Picoloto, *Rapid Commun. Mass Spectrom.*, 2020, **34**, e8727.
- 129 X. Bu, T. Wang and G. Hall, *J. Anal. At. Spectrom.*, 2003, **18**, 1443.
- 130 D. Clases and R. Gonzalez de Vega, *Anal. Bioanal. Chem.*, 2022, **414**, 7337–7361.
- 131 M. Bonta and A. Limbeck, *J. Anal. At. Spectrom.*, 2018, **33**, 1631–1637.
- 132 D. Shindo and T. Oikawa, in *Analytical Electron Microscopy for Materials Science*, ed. D. Shindo and T. Oikawa, Springer Tokyo, Japan, 2002, ch. 4, pp. 81–102.
- 133 A. V. Girão, G. Caputo and M. C. Ferro, in *Compr. Anal. Chem.*, ed. T. A. P. Rocha-Santos and A. C. Duarte, Elsevier, 1st edn, 2017, vol. 75, pp. 153–168.
- 134 D. Son, S. Cho, J. Nam, H. Lee and M. Kim, *Polymers*, 2020, **12**, 1053.
- 135 L. S. Birnbaum and F. S. Daniele, *Environ. Health Perspect.*, 2004, **112**, 9–17.
- 136 N. S. Allen and M. Edge, *J. Vinyl Addit. Technol.*, 2021, **27**, 211–239.
- 137 X. Llovet, A. Moy, P. T. Pinard and J. H. Fournelle, *Prog. Mater. Sci.*, 2021, **116**, 100673.
- 138 H.-K. Kim, H.-Y. Ha, J.-H. Bae, M. K. Cho, J. Kim, J. Han, J.-Y. Suh, G.-H. Kim, T.-H. Lee, J. H. Jang and D. Chun, *Sci. Rep.*, 2020, **10**, 13699.
- 139 M. Tiwari, S. K. Sahu, T. Rathod, R. C. Bhangare, P. Y. Ajmal, V. Pulhani and A. Vinod Kumar, *Trends Environ. Anal. Chem.*, 2023, **40**, e00221.
- 140 N. Saadatkhah, A. Carillo Garcia, S. Ackermann, P. Leclerc, M. Latifi, S. Samih, G. S. Patience and J. Chaouki, *Can. J. Chem. Eng.*, 2019, **98**, 34–43.
- 141 C. Schick, *Anal. Bioanal. Chem.*, 2009, **395**, 1589–1611.
- 142 J. Epp, in *Materials characterization using nondestructive evaluation (NDE) methods*, Elsevier, 2016, pp. 81–124.
- 143 A. A. Bunaciu, E. G. Udriștioiu and H. Y. Aboul-Enein, *Crit. Rev. Anal. Chem.*, 2015, **45**, 289–299.
- 144 A. Ali, Y. W. Chiang and R. M. Santos, *Minerals*, 2022, **12**, 205.
- 145 B. H. Stuart, *Infrared spectroscopy: fundamentals and applications*, John Wiley & Sons, 2004.
- 146 S. Materazzi and S. Vecchio, *Appl. Spectrosc. Rev.*, 2013, **48**, 654–689.
- 147 T. Hatakeyama and F. i. Quinn, *Thermal analysis: fundamentals and applications to polymer science*, Wiley, 1999.
- 148 C. A. Smith, *Polym. Test.*, 2016, **52**, 234–245.

